Combining Weak Lensing and Galaxy Light Polarization

Stamou, Chrisostomos

Combining Weak Lensing and Galaxy Light Polarization

Leiden Institute of Physics

Universiteit Leiden

Stamou Chrisostomos-Panagiotis

Student ID: s2917432

LION Supervisor: *Dr. M. Schaller*

Extenral Supervisor: *Prof. dr. K.H. Kuijken*

Leiden, The Netherlands

March 1, 2022

Contents

Abstract

The present thesis investigates how galaxy light polarization can be used to improve weak lensing measurements. The optical light we detect from disk galaxies scatters dust, introducing this way a polarization which affects the galaxy's appearance. This polarization is not affected by lensing and it can thus reveal information on the unlensed galaxy shape, information which is otherwise inaccessible. Bearing this information in mind alongside the knowledge that weak lensing is inherently very noisy , we study how we can optimally combine shear and polarization to alleviate some of the shape noise. We begin by introducing the basics of weak lensing and polarization and then, we construct the optimal estimator for shear, by making the crucial assumption that polarization is correlated to the intrinsic galaxy ellipticity. Afterwards, we put this estimator to work by means of numerical simulations and we find that if polarisation and intrinsic ellipticity are correlated the variance of the optimal estimator is smaller than the variance of the usual one. Afterwards, we use the KiDS-450 mock source catalogues provided by SLICS and we measure shear correlation functions by using the optimal estimator we derived and the usual estimator which is averaging the observed ellipticity for each galaxy. We find that the optimal estimator is less noisy than the usual one, and the more correlated polarisation and intrinsic ellipticity are, the less the noise of the optimal estimator, *i.e.* the more information polarisation brings to weak lensing measurements. The codes used for all calculations are publicly available via `https://github.com/Chrisostomos-Stamou/Combining-Weak-Lensing-and-Galaxy-Light-Polarisation`.

1 Introduction

1.1 Outline of the Thesis

We start by an introductory section, where we make a brief review of the concept of gravitational lensing and then we focus on weak lensing which is a versatile and powerful probe for cosmology. Then, we mention the challenges in measuring weak lensing which is a noisy effect, and we introduce the concept of polarization as a way to alleviate some of the noise. In Chapter 2, we discuss in detail weak lensing and how it is related to Cosmology. Specifically, we start by deriving the basic equations for lensing and then we focus on weak lensing by galaxy clusters and cosmic shear. We present a detailed analysis and all equations are explicitly derived. In the end of this chapter, we make the connection to Cosmology and demonstrate how cosmological parameters are constrained. We then proceed in Chapter 3, where we combine polarization and weak lensing, by constructing an optimal estimator for measuring shear. Our goal for this estimator is to yield less noise than the usual one which includes only the observed ellipticity and not polarization. We then put this estimator to work by means of numerical simulations using Python. In Chapter 4, we use the KiDS mock source catalogues provided by the SLICS project `https://slics.roe.ac.uk/` for measuring the optimal estimator we constructed in Chapter 3 and we compare it to the usual one in order to test the effect of polarisation to weak lensing measurements. Afterwards, we measure shear correlation functions by using the optimal and the usual estimators and we investigate which one brings less noise to the measurement of shear. In the final chapter 5 we present a summary of the document and our results.

1.2 Weak Gravitational Lensing: A powerful probe for Cosmology

Gravitational lensing is the phenomenon where the trajectory of a light ray is bended when the light ray passes close to a gravitational field. A simple illustration of this concept is presented in figure 1. A light ray emitted by a star travelling in a straight line, is deflected by an angle $\hat{\alpha}$ when the ray grazes the surface of the Sun. The separation between the light ray and the massive object (*lens*)- in this case, the Sun- is called the *impact parameter* and here is equal to the radius of the Sun. The formula for the deflection angle can be easily found[1] by using Newtonian gravity alongside the assumption that the lens is a point mass, and the result is [1, 2, 3, 4]

$$\hat{\alpha} = \frac{2GM}{c^2 R} \tag{1.1}$$

Thus, in the general case of whichever object that acts as a lens with a mass M, measuring the deflection angle given that we can also measure the impact parameter, implies measuring the mass of the lens. In the general case of extended lenses, **gravitational lensing measures the mass distribution!**

[1] We shall also present the derivation in Chapter 2

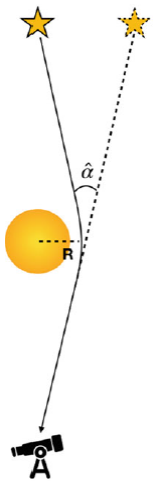

Figure 1: A simple manifestation of gravitational lensing:a light ray emitted from a star is deflected by an angle $\hat{\alpha}$ when it grazes the surface of the Sun. (Source: This figure is taken by [1])

The hisorical importance of gravitational lensing lies in the fact that it provided the first ever successful test of Einstein's General Relativity (GR). It turns out that in GR the expression for the deflection angle is the same as in (1.1), multiplied by a factor of two([1, 2, 3, 5, 6, 7, 8, 9, 10]):

$$\hat{\alpha} = \frac{4GM}{c^2 R} \tag{1.2}$$

It was this factor of two that Eddington used in his solar eclipse expedition (see figure 2) in 1920 [11] and proved that there is a new theory for gravity.

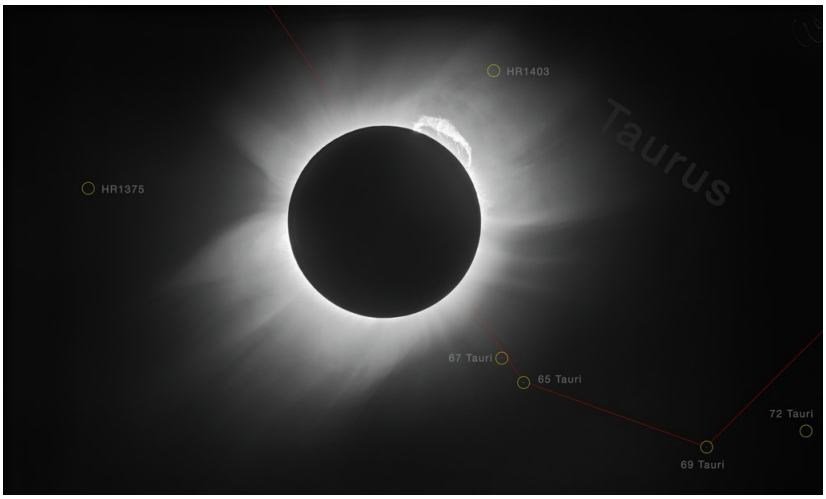

Figure 2: Digital restoration of a copy of one of the plates of the Eddington expedition on the island of Principe, performed as a part of the Heidelberg Digitalized Astronomical Plates project (see: `https://www.eso.org/public/images/potw1926a/`).

The effect of gravitational lensing is to distort the images of a source. Imagine an extended circular source emitting light rays that are deflected due to the presence of the gravitational field generated by a number of lenses. Adding up all these deflections result to a distorted image that can be magnified, de-magnified, squeezed or stretched along some preferred directions. This whole distortion is described by two quantities, the **convergence**, κ, and **shear**, γ. The effect of those is presented on figure 3. Both convergence and shear depend on the second spatial derivative of the

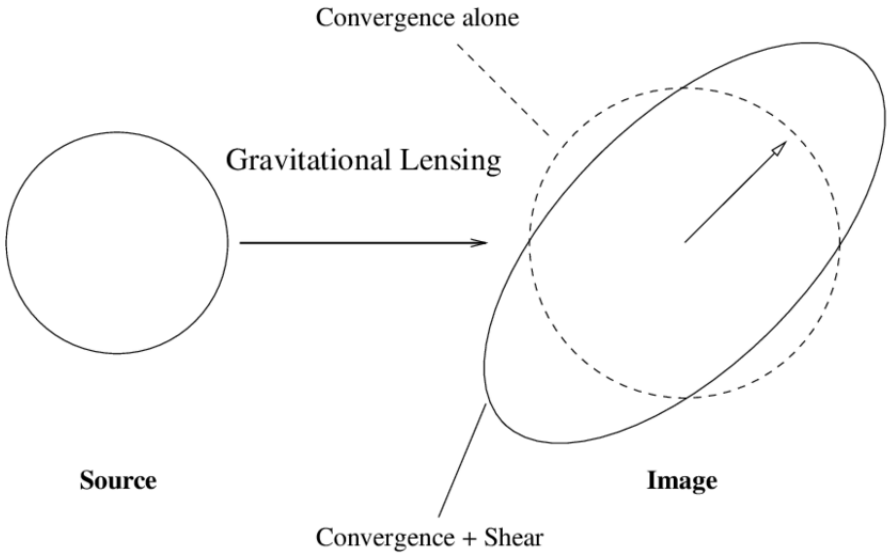

Figure 3: The effect of lensing on a circular source. Convergence is an isotropic distortion which preserves the shape of the source and shear is an anisotropic distortion that changes the shape by squeezing it or stretching it along preferred directions [12].

lensing potential (we shall present the derivation in Chapter 2). Specifically for convergence, it is defined as the Laplacian of the potential and hence it is directly connected to the surface density of the mass distribution via the Poisson equation. Depending on the values of κ and γ, we distinguish three different cases of gravitational lensing:

- **Strong Lensing:** Lenses in which both κ and γ are of order 1, produce strong distortions and multiple images. The first observation of strong lensing occurred in 1979 by Walsh *et al.* who detected a double-imaged quasar lensed by a galaxy [13]. Strong lensing is used to constrain the mass profile of lenses and it also has a cosmological application, since the Hubble constant can be inferred by measuring time delays between the images [14, 15].

- **Microlensing:** A case of strong lensing by moving stars. It was first detected by Irwin *et al.* [16] and it has a lot of important astrophysical applications, such as detecting exoplanets and putting constrains on the nature of Dark Matter.

- **Weak Lensing (WL):** Both shear and convergence are much smaller than 1. WL is a very slight distortion and does not produce multiple images. It occurs when emitted light rays from

background objects cross intervening foreground structures that induce weak gravitational fields. Such lensing occurs around every massive object, but the effect is too small to be measured for one single source. Therefore, weak lensing manifests itself when one performs a statistical analysis of the distortion of the shapes of a large number of source galaxies. It only relies on the physics of gravity and not on the composition of the object generating the gravitational field, consisting this way a versatile probe to constrain dark energy and dark matter, *i.e.* cosmology. WL was first detected in 1990 by Tyson *et al.* [17] and since then, it became a rapidly evolving field. Missions like CFHTLenS [18, 19], the Kilo Degree Survey (KiDS) [20, 21] and the Dark Energy Survey (DES) [22] have put constrains on cosmology and there is a lot more to come with future missions like EUCLID, Legacy Survey of Space and Time (LSST) and Dark Energy Spectroscopic Instrument (DESI) which will cover even larger areas of the sky and provide us with more data.

In the present thesis we are interested in WL as a probe for cosmology, and hence we shall not discuss further the strong lensing and the microlensing cases. Let us hence proceed by making the connection between cosmology and WL.

Connection to Cosmology

We've already stated that WL is measured by performing a statistical analysis of the distortion of the shapes of a large number of source galaxies. Let us describe this in a more detailed way. According to the intrinsic way that the sky works, galaxies are randomly oriented on the sky and their shapes are uncorrelated. Imagine now that we have a catalogue of galaxies and we see in this catalogue that there is a preferred alignment in the shape of the galaxies (right side of figure 4) and that they are not randomly oriented (left side of 4).

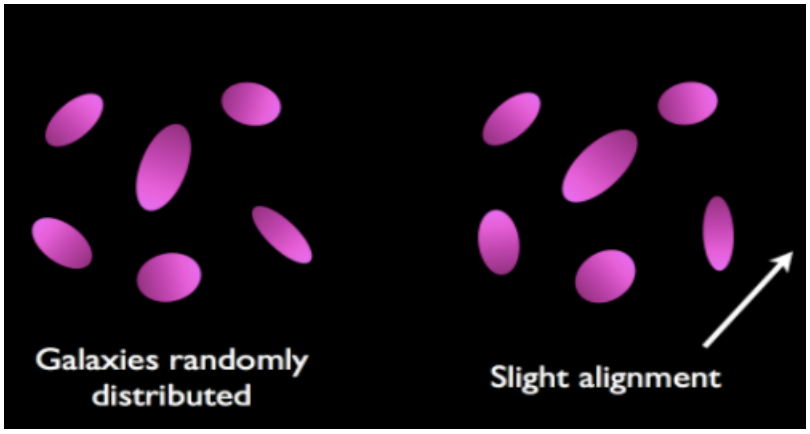

Figure 4: Left side: Galaxies that are randomly oriented and their shapes are uncorrelated. Right side: A present slight alignment in the orientation of the galaxies resulting in a correlation between the shapes. (source: `http://rcslens.org/public/what-gravitational-lensing`)

This preferred alignment that we see is the key-point here. It is shear that introduces this preferred alignment and what we observe is not the original shape of the source galaxy, but a result of WL and this is how WL is detected. This case is what we call **weak lensing by clusters**. The applications of WL by clusters are many and yield useful information. One application is to examine

the physical properites of clusters [23, 24, 25, 26, 27, 28, 29] Another set of applications is to study galaxies behind clusters where clusters are used as *cosmic telescopes* and their magnification makes distant galaxies bigger and brighter and hence easier to observe [3, 30, 31].

WL by clusters has of course an important application on providing constrains on Cosmology. The intensity of lensing effects depends on distances between the source and the observer, the lens and the observer, and between the lens and the source. These distances in an expanding Universe are comoving distances and hence lensing depends on the geometry of the Universe which eventually constrains cosmological parameters. A basis for putting constraints on Cosmology was provided by the MAssive Cluster Survey (MACS) [32] when a project titled "Weighing the Giants" used 51 clusters from MACS [33, 34, 35, 36]. and provided constrains on σ_8, Ω_m the neutrino masses and dark energy. An example of such constrains given by Mantz *et al.* [36] is shown in figure 5.

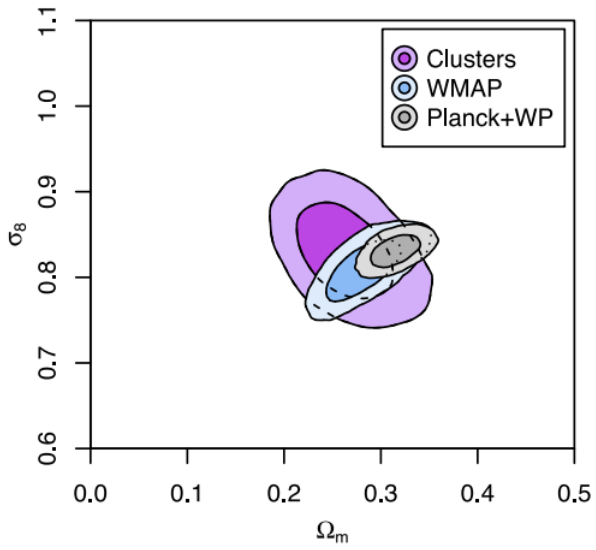

Figure 5: Constrains on σ_8 and Ω_m using the paper's data and comparing them to the results from *WMAP* and [37] and Planck + WP results [38].

WL by clusters is a case where a single object such as a galaxy cluster is responsible for the deflection light. However, this is not the only case. The light emitted from background sources is travelling in an inhomogeneous Universe and it's deflected by the intervening Large Scale Structure (LSS). As it is shown in figure 6, light rays emitted from three different sources are deflected many times from LSS until they reach to the observer. This effect is known as **Weak Lensing from Large Scale Structure**, or ***Cosmic Shear***. Therefore, cosmic shear is a probe of the LSS of the Universe and it can measure the distribution of dark matter along the line of sight. Observing cosmic shear and extracting information from it, goes like this: first, one has to measure galaxy shapes, then to determine how the source galaxies are distributed in redshift and then measure shear correlation functions. These functions are connected to the matter power spectrum by LSS and hence Cosmology is constrained.[2]

[2]This whole process will be discussed in depth in Chapter 2.

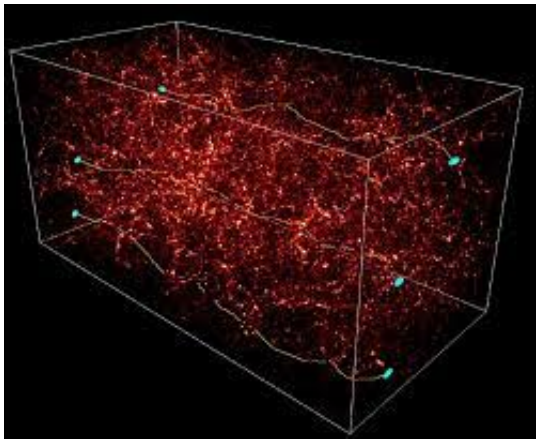

Figure 6: Demonstration of cosmic shear. Light rays are continuously deflected along the line sight due to the intervening LSS. Credits: CFHT team `https://www.cfht.hawaii.edu/News/Lensing/`

Comsic shear was first observed in 2000 [39, 40, 41] and ever since there have been efforts to measure cosmic shear over many hundreds of square degrees. Such missions are[3] the KiDS [42], DES [43] and the Hyper Suprime-Cam Subaru Strategic Program (HSC-SSP) [44].

It is obvious from what we have discussed above that the field of gravitational lensing is a rapidly evolving one and has thus far provided us with a lot of important information about our cosmos. WL is undoubtedly the most versatile application of gravitational lensing since it can measure the masses of individual massive galaxy clusters, average masses of ensembles of objects and the statistics of the matter distribution, but it is also the least precise which brings us to the next section.

1.3 Challenges in Shear Measurements and Polarization

Measuring cosmic shear is not an easy task. Distortions from Earth's atmosphere and telescope optics, noise from photon counts and detector read noise make WL an inherently very noisy effect. Another challenge in measuring shear is the intrinsic ellipticity of the source, which is typically much larger than the shear we're interested in. In addition, there is the effect of the Point Spread Function (PSF), which describes how a point source is smeared by the telescope optics, the telescope guiding, the several steps involved in the data reduction process, and the atmospheric turbulence. Of course, there have been developed tools to deal with these challenges, but we still realise that any extra information that can be brought to bear on the shear measurement is more than welcome.

The idea on this project, is to consider the polarization of galaxy light as an extra information on WL measurements. Optical light detected by disk galaxies contains information on the stellar distribution and dust. Besides extinction, dust also scatters light, an important effect that affects the galaxy's appearance. One of the manifestations of this scattering is polarization [45, 46] . The

[3]These missions are still releasing data and the citated articles are about the first release.

key-point here, is that the polarized light is not affected by lensing (see figure 7) and hence it could contain information on the unlensed galaxy shape, *i.e.* the intrinsic ellipticity. A WL survey measures the observed galaxy ellipticity, which when averaged is equal to the shear. If polarization and intrinsic ellipticity are correlated, measuring the degree of polarization for the same galaxies used in the WL survey could bring additional information on WL measurements and alleviate some of the shape noise.

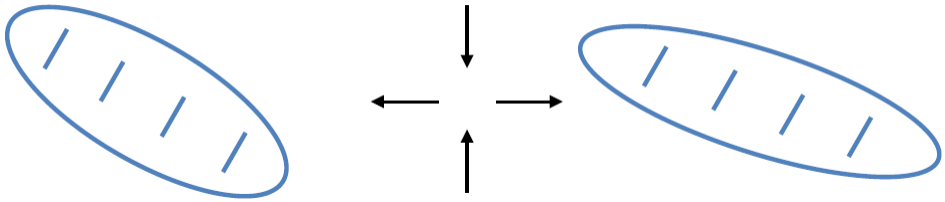

Figure 7: Polarization in not affected by lensing. The blue vertical lines represent polarization, which is aligned with the minor axis. On the left side, we see the original shape of the galaxy and on the right side, we see its distortion after being lensed. The lensing stretched the ellipse along the x-axis and squeezed it along the y-axis, but polarization is unaffected and is still aligned with the minor axis.

Our ultimate technical goal in this project is to construct an optimal estimator for measuring shear correlation functions that will include polarisation. Once we construct this estimator, we can compare its variance to the variance of the usual one and test which one is less noisy.

2 Weak Lensing and Cosmology

We start by deriving the very basics of lensing (section 2.1), *i.e.* the deflection angle formula and the lens equation and then we discuss the second-order effect of lensing which is to distort images, a phenomenon described by shear and convergence. Afterwards, we restrict our discussion to WL and we start by studying weak lensing by galaxy clusters (section 2.2), where we discuss how shear is inferred from galaxy shapes and define the quantities measured from a WL survey. We then proceed to the Cosmic shear case (section 2.3) and we start by setting the basis which is studying the propagation of light in an inhomogeneous Universe. Once this is done, we re-define the basic lensing quantities and we finally make the connection to cosmology (section 2.4) via the shear correlation functions. We notice that our goal is to explain the concepts involved and make clear how the mathematical expressions are derived and hence our discussion is more "theoretical" and we don't focus on observational technicalities.

2.1 Basics of Lensing

The most important quantity in gravitational lensing is of course the deflection angle. We will derive the formula for the deflection angle for three different cases:

- *Newtonian gravity*
- *Minkowski spacetime* (adequate for Solar System and other well-localised mass inhomogeneities)
- *Friedmann-Robertson-Walker spacetime*[4] (corresponds to cosmological scales)

Newtonian gravity

We have already mentioned that for a point-mass lens in the context of Newtonian theory, the deflection angle is given by (1.1). Let us now prove this. Consider a light ray passing near to a point-mass M and deflected by angle $\hat{\alpha}$, as it is shown in figure 8.

The light ray when it "feels" the presence of the gravitational field is accelerated by:

$$a = \frac{F}{m} = \frac{1}{m}\frac{GMm}{r^2} \Rightarrow a = \frac{GM}{r^2} \tag{2.1}$$

The deflection angle is defined as the fraction of the change in the velocity, Δv, over the speed of light c:

$$\hat{\alpha} = \frac{\Delta v}{c} \tag{2.2}$$

[4]This case will be discussed in section 2.3

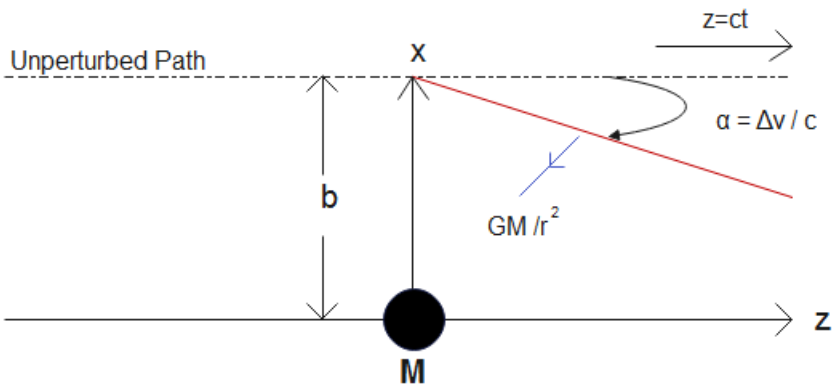

Figure 8: Deflection of a light ray due to the presence of a gravitational field generated by a point-mass M.

and Δv is the integral of the acceleration. Acceleration is a vector with components on the x-axis and on z-axis. Applying some basic trigonometry, we get by combining (2.1) and (2.2) that:

$$\begin{pmatrix}\Delta v_z\\ \Delta v_x\end{pmatrix} = \int_{-\infty}^{+\infty}\begin{pmatrix}a_z\\ a_x\end{pmatrix}dt = -\int_{-\infty}^{+\infty}\frac{GM}{(x^2+z^2)^{3/2}}\begin{pmatrix}z\\ x\end{pmatrix}dt \tag{2.3}$$

The deflection is very small and hence we can evaluate the acceleration on the unperturbed path, which is described by:

$$x(t) = b \qquad \& \qquad z(t) = ct \tag{2.4}$$

Substituting (2.4) into (2.3) yields:

$$\begin{pmatrix}\Delta v_z\\ \Delta v_x\end{pmatrix} = -\int_{-\infty}^{+\infty}\frac{GM}{(b^2+c^2t^2)^{3/2}}\begin{pmatrix}ct\\ b\end{pmatrix}dt \tag{2.5}$$

The integrals are easily calculated by a change of variables and the result is:

$$\begin{pmatrix}\Delta v_z\\ \Delta v_x\end{pmatrix} = -\frac{2GM}{bc}\begin{pmatrix}0\\ 1\end{pmatrix} \tag{2.6}$$

This is an expected result, since the deflection occurs along the vertical x-axis. Notice that the minus sign is just a matter of our choice of setup and we can neglect it by making a sign convention. Therefore, the deflection angle (2.2) is given by:

$$\boxed{\hat{\alpha} = \frac{2GM}{bc^2}} \tag{2.7}$$

Deflection angle in Minkowski space

Let us now consider the more general case of light rays propagating through a Minkowski space, which is characterised by the following famous metric:

$$\eta_{\mu\nu} = \begin{pmatrix} +1 & 0 & 0 & 0 \\ 0 & -1 & 0 & 0 \\ 0 & 0 & -1 & 0 \\ 0 & 0 & 0 & -1 \end{pmatrix} \tag{2.8}$$

We know from the field of geometrical optics, that the deflection of a light ray can be calculated by using Fermat's principle. The situation we have here is pretty much the same. The refractive index in our case that causes the light ray to bend is the gravitational potential. Therefore, we will apply Fermat's principle in order to derive the expression for the deflection angle.

Fermat's principle states that light will follow a path along which the travel time is external. Once the light ray is deflected, its velocity decreases and this is exactly the definition of the *refractive index*, n:

$$n = \frac{c}{v} \tag{2.9}$$

The travel time is then given by:

$$v = \frac{dl}{dt}$$

where dl is the path. Using (2.9) yields:

$$\frac{c}{n} = \frac{dl}{dt} \Rightarrow t = \int_A^B \frac{n}{c} dl \tag{2.10}$$

where the starting point A and the ending point B are fixed. Thus, we are searching for a path $\vec{x}(l)$ for which:

$$\delta \int_A^B n\left[\vec{x}(l)\right] dl = 0 \tag{2.11}$$

To proceed, we need to find an expression for the refractive index. The deflection in the trajectory of light occurs in a very small area compared to the total trajectory of the light ray. Therefore, we can safely assume that the lens is weak and hence the potential is small, *i.e.* $\frac{\Phi}{c^2} \ll 1$. This allows us to approximate the gravitational potential along the deflected path by the potential along the unperturbed path and it is a valid one, since in all cases of astrophysical interest the potential is indeed much smaller than c^2. A weak lens perturbs the metric as follows:

$$\eta_{\mu\nu} \to g_{\mu\nu} = \begin{pmatrix} \left(1+\frac{2\Phi}{c^2}\right) & 0 & 0 & 0 \\ 0 & -\left(1-\frac{2\Phi}{c^2}\right) & 0 & 0 \\ 0 & 0 & -\left(1-\frac{2\Phi}{c^2}\right) & 0 \\ 0 & 0 & 0 & -\left(1-\frac{2\Phi}{c^2}\right) \end{pmatrix} \tag{2.12}$$

and hence the light element is given by:

$$ds^2 = c^2\left(1+\frac{2\Phi}{c^2}\right)dt^2 - \left(1-\frac{2\Phi}{c^2}\right)(d\vec{x})^2 \tag{2.13}$$

Light rays follow null geodesics, *i.e.* $ds^2 = 0$ which yields:

$$c^2\left(1+\frac{2\Phi}{c^2}\right)dt^2 = \left(1-\frac{2\Phi}{c^2}\right)(d\vec{x})^2 \tag{2.14}$$

The light speed in the gravitational field is given by:

$$v = \frac{|d\vec{x}|}{dt} = c\sqrt{\frac{1+\frac{2\Phi}{c^2}}{1-\frac{2\Phi}{c^2}}} \tag{2.15}$$

Taylor expanding the terms in the square root yields:

$$v \simeq c\left(1+\frac{2\Phi}{c^2}\right) \tag{2.16}$$

Inserting (2.16) into the definition of the refractive index (2.9) and performing once again a Taylor expansion yields:

$$\boxed{n \simeq 1 - \frac{2\Phi}{c^2}} \tag{2.17}$$

Now that we have the expression for the refractive index, the path $\vec{x}(l)$ can be obtained from (2.11). We choose a parameter λ that describe the curve:

$$dl = \left|\frac{d\vec{x}}{d\lambda}\right| d\lambda \tag{2.18}$$

and (2.11) becomes:

$$\delta\int_A^B n\left[\vec{x}(l)\right] dl = 0 \Rightarrow \delta\int_{\lambda_A}^{\lambda_B} n\left[\vec{x}(l)\right]\left|\frac{d\vec{x}}{d\lambda}\right| d\lambda = 0 \tag{2.19}$$

We have a problem of variations and hence the easiest way to solve it is via the Euler-Lagrange equations:

$$\frac{d}{d\lambda}\frac{\partial\mathscr{L}}{\partial\dot{\vec{x}}} - \frac{\partial\mathscr{L}}{\partial\vec{x}} = 0 \tag{2.20}$$

where $\mathscr{L}$ is the Lagrangian which can be easily read off (2.19):

$$\mathscr{L}(\vec{x}, \dot{\vec{x}}, \lambda) = n\left[\vec{x}(l)\right] \left|\frac{d\vec{x}}{d\lambda}\right| \tag{2.21}$$

and a dot represents a derivative with respect to the parameter λ. Substituting this Lagrangian into (2.20) yields:

$$\frac{d}{d\lambda}\left(n\frac{\dot{\vec{x}}}{|\dot{\vec{x}}|}\right) - |\dot{\vec{x}}|\frac{\partial n}{\partial \vec{x}} = 0 \tag{2.22}$$

The vector $\dot{\vec{x}}$ is tangent to the curve and we can normalise its norm by a suitable choice of λ. Therefore, we write

$$|\dot{\vec{x}}| = 1 \qquad \& \qquad \vec{e} \equiv \dot{\vec{x}} \tag{2.23}$$

Taking these considerations into account, the equation of motion (2.22) becomes:

$$\frac{d}{d\lambda}\left(n\vec{e}\right) - \vec{\nabla} n = 0$$

$$\Rightarrow \frac{dn}{d\lambda}\vec{e} + n\frac{d\vec{e}}{d\lambda} - \vec{\nabla} n = 0$$

$$\Rightarrow \frac{dn}{d\vec{x}}\frac{d\vec{x}}{d\lambda}\vec{e} + n\dot{\vec{e}} - \vec{\nabla} n = 0$$

$$\Rightarrow n\dot{\vec{e}} + \vec{e}\left[\left(\vec{\nabla} n\right)\cdot\vec{e}\right] - \vec{\nabla} n = 0$$

$$\Rightarrow n\dot{\vec{e}} = \vec{\nabla} n - \vec{e}\left[\left(\vec{\nabla} n\right)\cdot\vec{e}\right] \tag{2.24}$$

The second term on the right-hand-side (*r.h.s.*) is the derivative along the light path and hence we realise that:

$$\vec{\nabla}_{\perp} n = \vec{\nabla} n - \vec{e}\left[\left(\vec{\nabla} n\right)\cdot\vec{e}\right] \tag{2.25}$$

Thus, equation (2.24) is simplified as:

$$\dot{\vec{e}} = \frac{1}{n}\vec{\nabla}_{\perp} n = \left(1 + \frac{2\Phi}{c^2}\right)\left(-\frac{2}{c^2}\vec{\nabla}_{\perp}\Phi\right)$$

where on the second equality we used (2.17). Keeping only first order terms to Φ we obtain:

$$\boxed{\dot{\vec{e}} \equiv \frac{d^2\vec{x}}{d\lambda^2} = -\frac{2}{c^2}\vec{\nabla}_\perp \Phi} \tag{2.26}$$

This equation describes how a light ray is curved away from a straight line in a perturbed Minkowski spacetime. The total deflection angle can now be easily obtained, since it is the integral over $-\dot{\vec{e}}$ along the light path:

$$\boxed{\hat{\alpha} = \vec{e}_{in} - \vec{e}_{out} = \frac{2}{c^2}\int_{\lambda_A}^{\lambda_B} \vec{\nabla}_\perp \Phi d\lambda} \tag{2.27}$$

Notice that if we use the potential of a point mass, *i.e.* $\Phi = -GM/r$, we recover the expression (2.7). multiplied by two because this is a relativistic treatment.

Let us now proceed by deriving the **lens equation**. Consider the setup presented in figure 9. A source emits a light ray that is constantly deflected by intervening lenses and we wish to find expression for the angle position of the source, because in reality we measure angles.

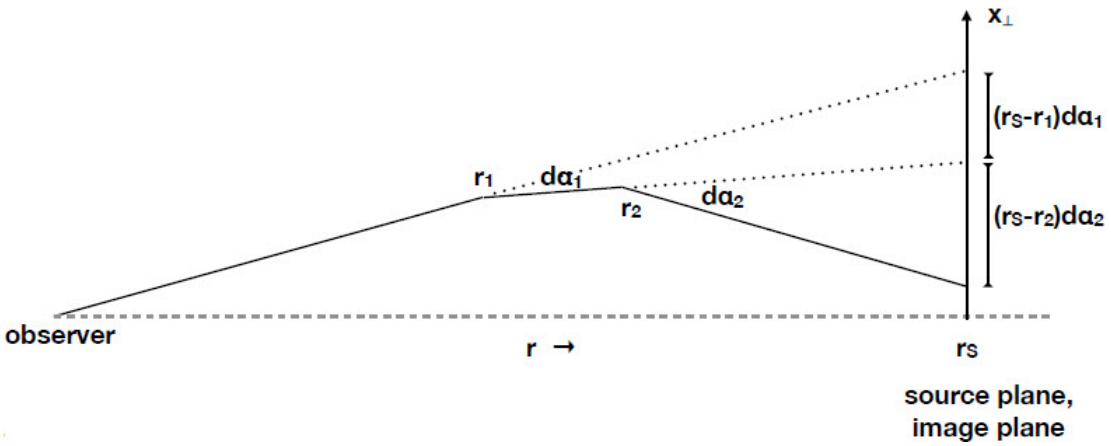

Figure 9: A source emits a light ray that is constantly deflected by intervening lenses.

The distance between the observer and the source is denoted by r_s and the distance between each lens and the observer is denoted by r. We wish to find an expression for the source position, $\delta\vec{x}_\perp$. If we consider the case of one lens, say the one at distance r_1, then:

$$\sin(d\alpha_1) \simeq d\alpha_1 = \frac{\delta x_\perp}{r_s - r_1} \Rightarrow \delta x_\perp = (r_s - r_1)\, d\alpha_1 \tag{2.28}$$

where we used the small-angle approximation, since the deflection is small. Thus, for every possible lens between the observer and the source, the latter equation becomes:

$$\delta\vec{x}_\perp = \int_0^{r_s} (r_s - r)\, d\vec{\alpha} \tag{2.29}$$

Using the expression we found for the deflection angle (2.27), we get:

$$\delta\vec{x}_\perp = \int_0^{r_s} (r_s - r)\,\frac{d\vec{\alpha}}{dr}dr = \frac{2}{c^2}\int_0^{r_s} dr\,(r_s - r)\,\vec{\nabla}_\perp\Phi$$

Hence, the angle position of the source is given by dividing the latter equation by r_s, and this is the **lens equation**:

$$\boxed{\delta\vec{\theta} \equiv \vec{\theta}_{unlensed} - \vec{\theta}_{lensed} = -\frac{2}{c^2}\int_0^{r_s} dr\frac{(r_s - r)}{r_s}\vec{\nabla}_\perp\Phi} \tag{2.30}$$

Let us proceed by making some definitions that will simplify the above expressions. The gravitational field generated by the lens is in general a mass with density $\rho(x, y, z)$ and the Poisson equation is:

$$\nabla^2\Phi = 4\pi G\rho \tag{2.31}$$

Integrating along the line of sight coordinate z yields:

$$4\pi G\Sigma(x, y) \equiv 4\pi G\int dz\rho(x, y, z) = \int dz\nabla^2\Phi = \vec{\nabla}\cdot\int dz\vec{\nabla}\Phi = \vec{\nabla}_\perp\cdot\int dz\vec{\nabla}_\perp\Phi \tag{2.32}$$

where $\Sigma(x, y)$ is the projected surface mass density and on the last integral, $d\Phi/dz$ integrates out. We can now define the projected lensing potential $\Psi(x, y)$ as:

$$\vec{\nabla}_\perp\Psi = \int dz\vec{\nabla}_\perp\Phi \tag{2.33}$$

and the two-dimensional Poisson equation becomes:

$$\nabla^2_{x,y}\Psi = 4\pi G\Sigma(x, y) \tag{2.34}$$

The lens equation can be simplified by defining the dimensionless lensing potential, $\psi(\theta)$, as:

$$\psi(\theta) = \frac{2}{c^2}\frac{r_{ls}}{r_l r_s}\Psi(r_l\theta) \tag{2.35}$$

where r_l is the distance between the observer and the lens, and $r_{ls} \equiv r_s - r_l$. Using this dimensionless definition, the lens equation becomes:

$$\delta\vec{\theta} = -\vec{\nabla}_{\vec{\theta}}\psi \tag{2.36}$$

The Poisson equation for the dimensionless potential is found by taking the gradient of (2.35) twice:

$$\vec{\nabla}_{\vec{\theta}}\psi = \frac{2}{c^2}\frac{r_{ls}}{r_s}$$

$$\Rightarrow \nabla^2_{\vec{\theta}}\psi = \frac{2}{c^2}\frac{r_l r_{ls}}{r_s}$$

$$\Rightarrow \boxed{\nabla^2_{\vec{\theta}}\psi = 2\frac{\Sigma}{\Sigma_{crit}}} \tag{2.37}$$

where we used equation (2.34) and we defined the *critical surface density* as:

$$\Sigma_{crit} = \frac{c^2}{4\pi G}\frac{r_s}{r_l r_{ls}} \tag{2.38}$$

The name critical arises because it defines the boundary over which strong lensing occurs. If $\Sigma_{crit} < \Sigma$ then strong lensing occurs.

Convergence and Shear

The first-order effect of lensing is to displace images from the source direction. The second-order effect is to **distort** the images because of the gradient of the displacement. Let us explain what exactly this means. We have already stated that the total path of a photon is much larger than the patch where the deflection occurs and hence the exchange of energy between the lens and the photon is very little. So little, that we can consider that it didn't actually exchange energy and hence surface brightness is conserved. However, the photon trajectory did get deflected by a tiny deflection angle. Thus, the photons emitted by an extended source are remapped from one surface to another- from the source plane to the image plane- but in doing so, they conserve their brightness. To describe this remapping, which is actually the distortion of the image, we are searching for a Jacobian matrix. Since the remapping occurs from the source plane to the image plane, this matrix will be:

$$A_{ij} = \frac{\partial \beta_i}{\partial \theta_j} \tag{2.39}$$

where $\beta \equiv \theta_{unlensed}$ and $\theta \equiv \theta_{lensed}$. This matrix is called the ***distortion matrix*** and we see from (2.36) that depends only on the second derivative of the lensing potential:

$$A_{ij} = \frac{\partial}{\partial \theta_j}\left(\theta_i - \partial_i \psi\right) = \delta_{ij} - \psi_{,ij} \tag{2.40}$$

where $\psi_{,ij} \equiv \frac{\partial^2 \psi}{\partial \theta_i \partial \theta_j}$. Hence, the distortion matrix is given by:

$$\boxed{A = \begin{pmatrix} 1-\psi_{,11} & -\psi_{,12} \\ -\psi_{,12} & 1-\psi_{,22} \end{pmatrix} = \begin{pmatrix} 1-\kappa-\gamma_1 & -\gamma_2 \\ -\gamma_2 & 1-\kappa+\gamma_1 \end{pmatrix}} \tag{2.41}$$

where we have defined the ***convergence***, κ and the ***shear***, γ_1, γ_2 as:

$$\kappa = \frac{1}{2}\left(\psi_{,11} + \psi_{,22}\right) = \frac{1}{2}\nabla^2\psi = \frac{1}{2}2\frac{\Sigma}{\Sigma_{crit}} = \frac{\Sigma}{\Sigma_{crit}} \tag{2.42}$$

$$\gamma_1 = \frac{1}{2}\left(\psi_{,11} - \psi_{,22}\right) \tag{2.43}$$

$$\gamma_2 = \psi_{,12} \tag{2.44}$$

Let us explain the reason behind the names convergence and shear. For that, let us write the distortion matrix in the following way:

$$\begin{pmatrix} d\beta_1 \\ d\beta_2 \end{pmatrix} = A \begin{pmatrix} d\theta_1 \\ d\theta_2 \end{pmatrix} = \begin{pmatrix} (1-\kappa-\gamma_1)\, d\theta_1 - \gamma_2 d\theta_2 \\ -\gamma_2 d\theta_1 + (1-\kappa+\gamma_1)\, d\theta_2 \end{pmatrix} \tag{2.45}$$

- Effect of Convergence

  If we set $\gamma_1 = \gamma_2 = 0$, equation (2.45) reduces to:

$$\begin{pmatrix} d\beta_1 \\ d\beta_2 \end{pmatrix} = \begin{pmatrix} (1-\kappa)\, d\theta_1 \\ (1-\kappa)\, d\theta_2 \end{pmatrix} = (1-\kappa) \begin{pmatrix} d\theta_1 \\ d\theta_2 \end{pmatrix} \tag{2.46}$$

  We see that the source is just rescaled by a factor of $1-\kappa$ and depending on the value of κ it is magnified or de-magnified (see figure 10). Thus, convergence is an isotropic distortion, since the shape of the source is conserved.

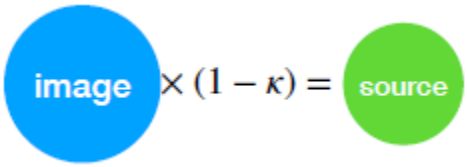

Figure 10: The effect of convergence. Source size is image size $\times\,(1-\kappa)$.

- Effect of Shear γ_1

  If we set $\kappa = \gamma_2 = 0$, equation (2.45) reduces to:

$$\begin{pmatrix} d\beta_1 \\ d\beta_2 \end{pmatrix} = \begin{pmatrix} (1-\gamma_1)\, d\theta_1 \\ (1+\gamma_1)\, d\theta_2 \end{pmatrix} \tag{2.47}$$

  We now see the distortion is not isotropic, since the shape of the source changes. There is a stretching by a factor of $(1-\gamma_1)$ along the x-axis and a stretching by a factor of $(1+\gamma_1)$ along the y-axis as it is shown in figure 11.

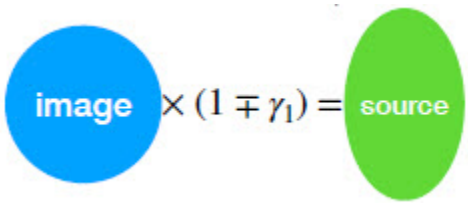

Figure 11: The effect of the shear component γ_1. Source is image, stretched by $(1-\gamma_1)$ in the x-axis and by $(1+\gamma_1)$ in y-axis.

- Effect of Shear γ_2

  If we set $\kappa = \gamma_1 = 0$, equation (2.45) reduces to:

$$\begin{pmatrix} d\beta_1 \\ d\beta_2 \end{pmatrix} = \begin{pmatrix} d\theta_1 - \gamma_2 d\theta_1 \\ -\gamma_2 d\theta_1 + d\theta_2 \end{pmatrix} \tag{2.48}$$

  The distortion in this case occurs along the positive/negative diagonal, as it is shown in figure 12.

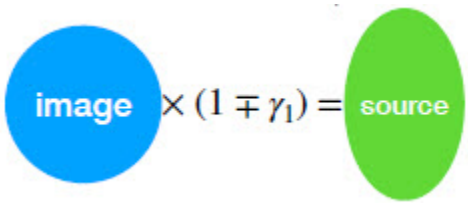

Figure 12: The effect of the shear component γ_2. Source is image, stretched by $(1-\gamma_2)$ along the positive diagonal and by $(1+\gamma_2)$ along the negative diagonal.

When both convergence and shear are non-zero, we have the effect shown in figure 3. Recall that surface brightness is preserved, which means that source area is changed and hence the flux is changed, or *magnified*. This magnification, μ, is obviously defined as the inverse of the determinant of the distortion matrix:

$$\mu = \frac{1}{det(A)} = \left[(1-\kappa)^2 - \left(\gamma_1^2 + \gamma_2^2\right)\right]^{-1} \tag{2.49}$$

Let us now see the effect of the distortion matrix on a circular source. All we have to do is to find the eigenvalues of this matrix. This is fairly easy and the result is:

$$\lambda_{1,2} = 1 - \kappa \pm \gamma \tag{2.50}$$

where $\gamma \equiv \sqrt{\gamma_1^2 + \gamma_2^2}$. These eigenvalues measure the amplification in the direction of the eigenvectors of the shear tensor and for an axisymmetric lens, they are tangentially and radially oriented:

$$\mu_t = \frac{1}{\lambda_t} = \frac{1}{1 - \kappa - \gamma} \tag{2.51}$$

$$\mu_r = \frac{1}{\lambda_r} = \frac{1}{1 - \kappa + \gamma} \tag{2.52}$$

The shear tensor is defined as:

$$\tilde{\Gamma} = \begin{pmatrix} \gamma_1 & \gamma_2 \\ \gamma_2 & -\gamma_1 \end{pmatrix} \tag{2.53}$$

Therefore, we can safely say that a circular source with radius R is mapped into an ellipse with semi-major, a and semi-minor, b, axes given by:

$$a = \frac{R}{1 - \kappa - \gamma} \qquad b = \frac{R}{1 - \kappa + \gamma} \tag{2.54}$$

The ellipticity is then given by:

$$\boxed{\epsilon = \frac{a - b}{a + b} = \frac{\gamma}{1 - \kappa}} \tag{2.55}$$

Let us sum-up what we've discussed so far. The effect of lensing is to distort the image of a source and this distortion is described by shear (anisotropic distortion) and convergence (rescaling of the source) which is directly connected to the mass density (see equation (2.42)). Ellipticity is a combination of shear and convergence and it is what we measure in WL surveys. As we shall soon see, this measurement eventually yields in measuring convergence, *i.e.* mass, and this is how WL is used to infer the mass distribution along the line of sight. From now on, we restrict our discussion solely to WL, where $\kappa, \gamma \ll 1$.

2.2 Weak Lensing by Galaxy Clusters

Lensing distorts circular sources to ellipses, with their major and minor axes pointing in the direction introduced by the eigenvectors of the shear tensor, with eigenvalues $\gamma = \sqrt{\gamma_1^2 + \gamma_2^2}$. It is convenient to define the *reduced shear* as:

$$g = \frac{\gamma}{1 - \kappa} \tag{2.56}$$

Then the ellipticity ((2.55)) is identical to the reduced shear:

$$\epsilon = g \tag{2.57}$$

Both shear and ellipticity-and hence the reduced shear as well- are spin-2 quantities, *i.e.* they rotate twice as fast as the coordinates, and it is usually convenient to express them in a complex form:

$$\gamma = \gamma_1 + i\gamma_2 \tag{2.58}$$

$$\epsilon = \epsilon_1 + i\epsilon_2 \tag{2.59}$$

$$g = g_1 + ig_2 \tag{2.60}$$

We realise that ellipticity measures a combination of shear and convergence and by measuring the ellipticity of images we can eventually infer the mass distribution of the lenses. Therefore, the starting point is to measure the ellipticity of galaxies. The main technique for that is via the surface brightness distribution. We begin by defining the image centroid, which is given by the first moment of the surface brightness:

$$\vec{\theta_0} = \frac{\int d^2\vec{\theta} I\left(\vec{\theta}\right) \vec{\theta}}{\int d^2\vec{\theta} I\left(\vec{\theta}\right)} \tag{2.61}$$

The shape of the image is determined by the second moment of the surface brightness, *i.e.* the quadrupole:

$$Q_{ij} = \frac{\int d^2\vec{\theta} I\left(\vec{\theta}\right) (\theta_i - \theta_{0i}) (\theta_j - \theta_{0j})}{\int d^2\vec{\theta} I\left(\vec{\theta}\right)} \tag{2.62}$$

which is a symmetric 2×2 tensor:

$$\tilde{Q} = \begin{pmatrix} Q_{11} & Q_{12} \\ Q_{12} & Q_{22} \end{pmatrix} \tag{2.63}$$

This tensor can be diagonalized and its eigenvectors define the principal axes of the surface brightness distribution. Therefore, the square of the length of the semi-major and semi-minor axes of the ellipse are reciprocal to the eigenvalues of the tensor $\tilde{Q}$. These can be easily found to be:

$$\lambda_+ = \frac{1}{2}\left[Q_{11} + Q_{22} + \sqrt{(Q_{11} - Q_{22})^2 + 4Q_{12}^2}\right] = \frac{1}{a^2} \tag{2.64}$$

$$\lambda_- = \frac{1}{2}\left[Q_{11} + Q_{22} - \sqrt{(Q_{11} - Q_{22})^2 + 4Q_{12}^2}\right] = \frac{1}{b^2} \tag{2.65}$$

Thus, an expression for ellipticity can be worked out by combining equations (2.64),(2.65) and (2.55):

$$|\epsilon| = \frac{\sqrt{(Q_{11} - Q_{22})^2 + 4Q_{12}^2}}{Q_{11} + Q_{22} + 2\sqrt{Q_{11}Q_{22} - Q_{12}^2}} \tag{2.66}$$

Since, $|\epsilon| = \sqrt{\epsilon_1^2 + \epsilon_2^2}$, the components can be easily found by comparison to equation (2.66):

$$\epsilon_1 = \frac{Q_{11} - Q_{22}}{Q_{11} + Q_{22} + 2\sqrt{Q_{11}Q_{22} - Q_{12}^2}} \tag{2.67}$$

$$\epsilon_2 = \frac{2Q_{12}}{Q_{11} + Q_{22} + 2\sqrt{Q_{11}Q_{22} - Q_{12}^2}} \tag{2.68}$$

Finally, the position angle of the ellipse gives the shear direction ϕ:

$$\tan(2\phi) = \frac{\epsilon_2}{\epsilon_1} = \frac{2Q_{12}}{Q_{11} - Q_{22}} \tag{2.69}$$

Thus, ellipticity is measured from the surface brightness distribution and this measurement yields the reduced shear. We should notice here that in practice, shape measurements are performed on pixelized images and hence the integrals in the definition of the surface brightness moments are substituted by summations.

The scalar nature of the lensing potential simplifies the situation since a single lens can only induce tangential and radial distortions. Therefore, it makes sense to redefine the shear components. We consider a rotated frame where the θ_1' axis passes through the image centroid and the lens center. Thus, we have a rotational transformation described by the rotation matrix:

$$R = \begin{pmatrix} \cos(\phi) & -\sin(\phi) \\ \sin(\phi) & \cos(\phi) \end{pmatrix} \tag{2.70}$$

where ϕ is the angle between the θ_1 and θ_1' axis. The shear tensor is then rotated as:

$$\tilde{\Gamma}' = R^T \tilde{\Gamma} R \tag{2.71}$$

and its components are easily found to be:

$$\gamma_1' = \gamma_1 \cos(2\phi) + \gamma_2 \sin(2\phi) \tag{2.72}$$

$$\gamma_2' = \gamma_1 \cos(2\phi) - \gamma_2 \sin(2\phi) \tag{2.73}$$

In order for only radial and tangential distortions to occur, the non-diagonal components of the shear tensor should be zero. Thus, we define the tangential, γ_t and the cross, $\gamma_\times$, shear components as:

$$\gamma_t = -\gamma_1' \qquad , \qquad \gamma_\times = -\gamma_2' \tag{2.74}$$

Tangential shear includes all the signal information and cross shear gives no signal. Detection of a non-zero cross shear component implies that there are systematic errors. An example of tangential and cross reduced shear measurements from a galaxy cluster (Umetsu *et. al* [47]) is shown in figure 13.

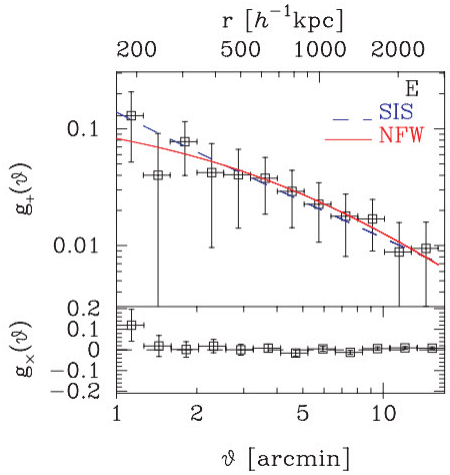

Figure 13: Tangential and cross reduced shear measurements from the A68 cluster. Top panel shows the measurement of the tangential reduced shear and bottom panel the measurement of the cross component. We see that the cross component gives no signal, as expected. The blue line represent the Singular Isothermal Sphere (SIS) lens model and the red line the Navarro-Frenk-White (NFW) halo model.

2.3 Weak Lensing from Large Scale Structure, *i.e.* Cosmic Shear

Before starting our discussion on WL from Large Scale Structure (LSS), let us first mention very briefly and generically what LSS is. Inflation produced the seed for inhomogeneities in the Universe which can eventually grow through gravitational instability. As long as these inhomogeneities are small, we can treat them as perturbations and study their evolution. This evolution depends on the wavelength of the perturbations and the era under consideration (matter era, radiation era, inflationary era, dark energy era). Perturbations with wavelengths larger than the Hubble radius, *i.e.* the distance at which the Hubble velocity is equal to the speed of light are called *superhorizon* perturbations and they can only evolve very slowly because objects are receding away from one another too fast and the dynamics among them is too little. Perturbations with wavelength smaller than the Hubble radius are called *subhorizon* perturbations and they can grow or damp faster. All of the structure that we can see today is going up to $100Mpc$, which corresponds to the radiation era. Subhorizon perturbations that propagate during the radiation era experience a logarithmic growth and when these modes enter the matter era, they grow linearly with respect to the scale factor. This evolution depends heavily on the cosmology of the Universe and it is what is measured by the *matter power spectrum* which is shown in figure 14. Eventually, perturbations will grow enough and they will become unstable and non-linear, which eventually will lead to their collapse and formation of haloes. For more information about the LSS and the matter power spectrum see the excellent cosmology notes from D. Baumann [48] or for a more comprehensive view see [49].

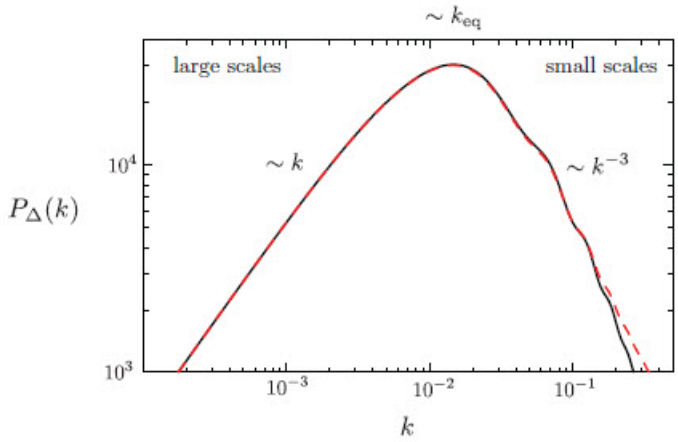

Figure 14: The matter power spectrum at redshift $z = 0$ in linear theory (solid line) and with non-linear corrections (dashed line).

WL by LSS, or *Cosmic Shear*, is the phenomenon where light rays emitted from distant background galaxies are deflected due to the whole intervening LSS standing between us and the galaxies. Measurement of this cosmic shear field, means measuring convergence because those two have the both power spectrum, and this is the connection point to cosmology. The power spectrum of convergence is directly connected to the matter power spectrum, as we shall prove, and this can hence constrain Cosmology. Therefore, our task is to reproduce the basic lensing equations for an expanding and inhomogeneous spacetime. In order to do so, we must start by studying the propagation of light in an inhomogeneous Universe (section 2.3.1), apply our findings to derive the deflection angle and

the lensing equation (section 2.3.2), and then derive the expressions for the convergence and the shear correlation functions (section 2.3.3). The connection to Cosmology is then shown in section 2.4. Before starting this whole process, let us first prove that shear and convergence have the same power spectrum. We start by writing shear and convergence in Fourier space:

$$\kappa = \frac{1}{2}\left(\psi_{,11} + \psi_{,22}\right) \Rightarrow \hat{\kappa} = -\frac{1}{2}\left(k_1^2 + k_2^2\right)\hat{\psi} \tag{2.75}$$

where by a hat we denote the Fourier transformed quantities. Doing the same for the complex shear given by (2.58),(2.43),(2.44):

$$\gamma = \frac{1}{2}\left(\psi_{,11} - \psi_{,22} + 2i\psi_{,12}\right) \Rightarrow \hat{\gamma} = -\frac{1}{2}\left(k_1^2 - k_2^2 + 2ik_1k_2\right)\hat{\psi} \tag{2.76}$$

Changing the coordinate system to polar coordinates where $k_1 = k\cos\phi$ and $k_2 = k\sin\phi$, the above expressions are written as:

$$\hat{\kappa} = -\frac{k^2}{2}\hat{\psi} \qquad , \qquad \hat{\gamma} = -\frac{k^2}{2}e^{2i\phi}\hat{\psi} \tag{2.77}$$

The power spectrum of a quantity α is defined as $P_\alpha = |\hat{\alpha}|^2$. So the mapping from shear to convergence, *i.e.* surface mass density, is just a rotation (factor $e^{2i\phi}$) in Fourier space and since amplitude is preserved:

$$|\hat{\kappa}(\vec{k})| = |\hat{\gamma}(\vec{k})| \tag{2.78}$$

which means that shear and convergence have the same power spectrum.

2.3.1 Propagation of light in an inhomogeneous Universe

We are generally considering light rays travelling through an inhomogeneous space. Therefore, a good starting point would be to consider a bundle of light rays emitted from a source and study the evolution of the shape of the bundle. We know from General Relativity that two light rays travelling in a curved spacetime experience the so-called geodesic deviation which is given by[5]

$$\frac{D^2\xi^a}{D\lambda^2} + R^a{}_{bcd}\xi^b\frac{dx^c}{d\lambda}\frac{dx^d}{d\lambda} = 0 \tag{2.79}$$

where $D/D\lambda$ is the intrinsic derivative, λ is an affine parameter describing the curve, ξ^a is the connection vector connecting the two light rays and $R^a{}_{bcd}$ is the Riemann tensor describing the curvature of spacetime which is what makes the light rays to eventually diverge.

[5]For a derivation of the geodesic deviation equation check [5].

Let us now study how the shape of the bundle evolves by following Schneider's notes [2]. Consider an observer O with 4-velocity U_0^μ obeying:

$$U_O^\mu U_{O\mu} = 1 \tag{2.80}$$

It is convenient to work in the eikonal approximation, where the wavevector is given by

$$\tilde{k}^\mu = \frac{dx^\mu}{d\lambda} \tag{2.81}$$

and the affine parameter λ is defined such that $\lambda = 0$ at O, λ increases along the backward light cone of O and $U_O^\mu \tilde{k}_\mu = -1$ at O. The physical wavevector k^μ of a photon depends on the light frequency as we know from wave mechanics,

$$k = \frac{\omega}{c} \tag{2.82}$$

and it is connected to $\tilde{k}^\mu$ via:

$$\tilde{k}^\mu = -\frac{c}{\omega_O} k^\mu \tag{2.83}$$

Let $\gamma^\mu(\vec{\theta}, \lambda)$ characterise the rays of a light beam with vertex at the observer O, such that θ is the angle between a ray and the fiducial ray characterised by $\gamma_0^\mu(\lambda) \equiv \gamma^\mu(\vec{0}, \lambda)$. We are interested in the vector connecting those two rays and hence we define the connection vector by,

$$Y^\mu(\vec{\theta}, \lambda) = \gamma^\mu(\vec{\theta}, \lambda) - \gamma_0^\mu(\lambda) \tag{2.84}$$

We can assume that the angle θ is small enough and hence the connection vector can be linearised with respect to θ. To do that, we notice that according to our definitions above, U_O^μ and $\tilde{k}^\mu$ define a two-dimensional plane perpendicular to both of them. This plane is tangent to the sphere of directions seen by the observer at O and we can hence span it by two orthonormal vectors E_1^μ and E_2^μ satisfying:

$$E_1^\mu E_{2\mu} = 0, \qquad E_j^\mu E_{j\mu} = -1, \qquad E_j^\mu \tilde{k}_\mu = E_j^\mu U_{O\mu} = 0 \tag{2.85}$$

where $j = 1, 2$. Taking all of the above into account, we can decompose the connection vector as:

$$Y^\mu(\vec{\theta}, \lambda) = -\xi_1(\vec{\theta}, \lambda) E_1^\mu - \xi_2(\vec{\theta}, \lambda) E_2^\mu - \xi_0(\vec{\theta}, \lambda) \tilde{k}^\mu \tag{2.86}$$

where $\vec{\xi}(\vec{\theta}, \lambda) = (\xi_1, \xi_2)$ describes the transverse separation of the two light rays, whereas ξ_0 allows for a deviation component along the beam direction. Since the connection vector is linear

to θ, then ξ should also be linear because of equation (2.86) and the choice of the affine parameter λ can reassure us that $d\vec{\xi}/d\lambda(\lambda = 0) = \vec{\theta}$. We can thus write the linear propagation equation as:

$$\vec{\xi}(\lambda) = \mathscr{D}(\lambda)\vec{\theta} \tag{2.87}$$

where the 2×2 matrix $\mathscr{D}$ satisfies the Jacobi equation:

$$\frac{d^2\mathscr{D}(\lambda)}{d\lambda^2} = \mathscr{T}(\lambda)\mathscr{D}(\lambda) \tag{2.88}$$

with boundary conditions,

$$\mathscr{D}(O) = 0 \qquad \& \qquad \frac{d\mathscr{D}}{d\lambda}(O) = \mathbb{I} \tag{2.89}$$

where $\mathbb{I}$ is the 2×2 identity matrix. The key-feature here is the matrix $\mathscr{T}(\lambda)$ in which the whole information about the shape of the bundle is encoded. Remember that the light rays are travelling through an inhomogeneous space and get deflected many times. Therefore, the shape of the bundle could be rescaled, stretched, squeezed or stay exactly the same with the latter being unlikely to ever happen. Therefore, the matrix $\mathscr{T}$ should include all these possible distortions. Starting by the isotropic case that the shape is rescaled, we see that this is actually the same with convergence and since it is an isotropic distortion it should be placed on the diagonal of the matrix. The anisotropic distortion, *i.e.* squeezing or stretching which is the same with shear should be placed in the off-diagonal elements. More precisely, the anisotropic distortion which we call *shear source*, is a complex number and hence its real part will be placed in the diagonal elements and its imaginary part in the off-diagonal elements. Taking all these into account, we see that the matrix $\mathscr{T}$ is actually a generalization of the distortion matrix (2.39) and is given by:

$$\mathscr{T}(\lambda) = \begin{pmatrix} \mathscr{R}(\lambda) + \Re[\mathscr{F}(\lambda)] & \Im[\mathscr{F}(\lambda)] \\ \Im[\mathscr{F}(\lambda)] & \mathscr{R}(\lambda) - \Re[\mathscr{F}(\lambda)] \end{pmatrix} \tag{2.90}$$

where $\mathscr{R}(\lambda)$ is the *convergence source* and $\mathscr{F}(\lambda)$ is the *shear source*.

Before we proceed, let us sum-up what we've done so far. We are interested in studying the evolution of the shape of a light bundle travelling in an inhomogeneous space. We proved that what characterises this shape is the matrix $\mathscr{T}$ which is usually called the *tidal optical matrix*. Therefore, our next step will be to apply this matrix in a Friedmann-Robertson-Walker (FRW) Universe-since we're interested in Cosmology- and derive the propagation of equation in such a spacetime.

We start by considering light propagation in an unperturbed FRW Universe and we'll then include the inhomogeneities. The metric for an FRW Universe is:

$$ds^2 = c^2dt^2 - a^2(t)\left(\frac{dr^2}{1 - Kr^2} + r^2d\theta^2 + r^2\sin^2\theta d\phi^2\right) \tag{2.91}$$

where $K = -1, 0, +1$ describes the curvature of the Universe and $a(t)$ is the scale factor. Depending

on the value of K and setting $dw = dr/\sqrt{1-Kr^2}$, the metric may be written as:

$$ds^2 = c^2dt^2 + a^2(t)\left[dw^2 + f_K^2(w)\Omega^2\right] \tag{2.92}$$

where $d\Omega$ is the solid angle and $f_K(w)$ is given by:

$$f_K(w) = \begin{cases} \frac{1}{\sqrt{K}}\sin\left(\sqrt{K}w\right) & \text{if } K > 0 \\ w & \text{if } K = 0 \\ \frac{1}{\sqrt{-K}}\sinh\left(\sqrt{-K}w\right) & \text{if } K < 0 \end{cases} \tag{2.93}$$

This metric is homogeneous and isotropic, which implying that anisotropic terms in the optical tidal matrix are equal to zero: $\mathscr{F}(\lambda) = 0$ and hence:

$$\mathscr{T}(\lambda) = \begin{pmatrix} \mathscr{R}(\lambda) & 0 \\ 0 & \mathscr{R}(\lambda)0 \end{pmatrix} \Rightarrow \mathscr{T}(\lambda) = \mathscr{R}(\lambda)\mathbb{I} \tag{2.94}$$

Using the Jacobi equation alongside the expression for $\vec{\xi}$, we see that the equation of motion for the transverse separation between neighbouring rays is given by:

$$\frac{d^2\vec{\xi}}{d\lambda^2} = \mathscr{T}\vec{\xi} \tag{2.95}$$

Substituting (2.92) into (2.93) we find:

$$\frac{d^2\vec{\xi}}{d\lambda^2} = \mathscr{R}(\lambda)\vec{\xi} \tag{2.96}$$

which is actually the same with the equation of geodesic deviation (2.79). Comparing these two, we can find an expression for λ in the eikonal approximation that we're working on and that is:

$$\mathscr{R}(\lambda) = -\frac{1}{2}R_{\mu\nu}(\lambda)\tilde{k}^{\mu}(\lambda)\tilde{k}^{\nu}(\lambda) \tag{2.97}$$

Let us hence proceed by finding an expression for $\mathscr{R}(\lambda)$. Notice that it includes the Ricci tensor and the "product" of the wavevectors. We also know that the wavevector is a null vector, *i.e.* $\tilde{k}^{\mu}\tilde{k}_{\mu} = g_{\mu\nu}\tilde{k}^{\mu}\tilde{k}^{\nu} = 0$. Ricci tensor can be written with respect to the metric tensor via the EInstein equations:

$$R_{\mu\nu} - \frac{1}{2}g_{\mu\nu}R + \Lambda g_{\mu\nu} = \frac{8\pi G}{c^4} \tag{2.98}$$

where R is the Ricci scalar, Λ is the cosmological constant and $T_{\mu\nu}$ is the energy-momentum tensor. Combining equations (2.97) and (2.98) we get:

$$\mathscr{R}(\lambda) = -\frac{1}{2}\left[\frac{8\pi G}{c^4}T_{\mu\nu}\tilde{k}^{\mu}\tilde{k}^{\nu} + \frac{1}{2}g_{\mu\nu}\tilde{k}^{\mu}\tilde{k}^{\nu} - \Lambda g_{\mu\nu}\tilde{k}^{\mu}\tilde{k}^{\nu}\right]$$

Using that $\tilde{k}^\mu$ is a null vector, the above expression reduces to:

$$\mathscr{R}(\lambda) = -\frac{4\pi G}{c^4} T_{\mu\nu} \tilde{k}^\mu \tilde{k}^\nu \tag{2.99}$$

Since we are working in an FRW Universe, the energy-momentum tensor describes a perfect fluid and is given by:

$$T_{\mu\nu} = \left(\rho + \frac{P}{c^2}\right) u_\mu u_\nu + P g_{\mu\nu} \tag{2.100}$$

where ρ is the density of the fluid, P is the pressure and $u^\mu = [c, 0, 0, 0]$ is the fluid's 4-velocity[6]. Since the spatial components of the 4-velocity are zero and $\tilde{k}^\mu$ is a null vector, the non-zero terms in (2.99) will be:

$$\mathscr{R}(\lambda) = -\frac{4\pi G}{c^4} \left(\rho + \frac{P}{c^2}\right) u_0 u_0 \tilde{k}^0 \tilde{k}^0 = -\frac{4\pi G}{c^4} \left(\rho + \frac{P}{c^2}\right) c^2 \tilde{k}^0 \tilde{k}^0 \tag{2.101}$$

Recall now equations (2.83) and (2.82). The frequency that the observer detects, ω_O is connected to the emitted frequency via the redshift:

$$\frac{\omega}{\omega_O} = 1 + z \tag{2.102}$$

Substituting this into (2.83) we find:

$$\tilde{k}^0 = -\frac{c}{\omega_O} \frac{\omega_O}{c} (1 + z) \Rightarrow \tilde{k}^0 = -(1 + z) \tag{2.103}$$

Therefore, equation (2.101) becomes:

$$\mathscr{R}(\lambda) = -\frac{4\pi G}{c^2} \rho \, (1 + z)^2 \tag{2.104}$$

where the density of the fluid ρ represents the matter density, which evolves as $\rho = \rho_0 a^{-3}$. Using the definition of the density parameter:

$$\Omega = \frac{\rho}{\rho_{crit}} \tag{2.105}$$

where the subscript zero denotes the present day value and $\rho_{crit} = 3H^2/(8\pi G)$ is the critical density of the Universe, we can rewrite the expression for $\mathscr{R}$ as:

$$\boxed{\mathscr{R}(\lambda) = -\frac{3}{2} \left(\frac{H_0}{c}\right)^2 \frac{\Omega_0}{a^5}} \tag{2.106}$$

[6]For a justification of why we consider a perfect fluid and how this expression occurs, check [5, 6, 7, 8, 9, 10]

Thus, the equation of motion for the transverse separation vector becomes:

$$\boxed{\frac{d^2\vec{\xi}}{d\lambda^2} = -\frac{3}{2}\left(\frac{H_0}{c}\right)^2 \frac{\Omega_0}{a^5}\vec{\xi}} \tag{2.107}$$

It will prove convenient to replace the affine parameter λ by the comoving distance-the distance that takes into account the expansion of the Universe- w. Therefore, we want to find the relation between w and λ. To this end, we start by considering the fact that light rays follow null geodesics and they are past directed. Applying this into the metric (2.92) yields:

$$cdt = -adw \tag{2.108}$$

We can further find a relation between λ and the scale factor by (2.83) and (2.103):

$$\tilde{k}^0 = \frac{cdt}{d\lambda} \Rightarrow d\lambda = -acdt$$

$$\Rightarrow d\lambda = -ac\frac{dt}{da}da \Rightarrow da = -\frac{H}{c}d\lambda \tag{2.109}$$

Notice here that we can rewrite (2.108) as:

$$cdt = -adw \Rightarrow c\frac{dt}{da}da = -adw \Rightarrow \frac{c}{\dot{a}}da = -adw$$

$$dw = -\frac{c}{a^2 H}da \tag{2.110}$$

where a dot represents a derivative with respect to time. Plugging in equation (2.109) yields:

$$d\lambda = a^2 dw \tag{2.111}$$

Let us sum-up here altogether the important relations between the parameters that we will use in the following derivations:

$$cdt = -adw \tag{2.112}$$

$$da = -\frac{H}{c}d\lambda \tag{2.113}$$

$$d\lambda = a^2 dw \tag{2.114}$$

Now that we know how dw and $d\lambda$ are connected, we can proceed in expressing $d/d\lambda$ and $d^2/d\lambda^2$ as derivatives with respect to the comoving distance.

$$\frac{d}{d\lambda} = \frac{dw}{d\lambda}\frac{d}{dw} \Rightarrow \boxed{\frac{d}{d\lambda} = \frac{1}{a^2}\frac{d}{dw}} \tag{2.115}$$

For the second derivative:

$$\frac{d^2}{d\lambda^2} = \frac{d}{d\lambda}\left(\frac{1}{a^2\frac{d}{dw}}\right) = \frac{d}{d\lambda}\left(\frac{1}{a^2}\right)\frac{d}{dw} + \frac{1}{a^2}\frac{dw}{d\lambda}\frac{d^2}{dw^2}$$

$$\Rightarrow \frac{d^2}{d\lambda^2} = \frac{da}{d\lambda}\left(\frac{-2}{a^3}\right)\frac{d}{dw} + \frac{1}{a^4}\frac{d^2}{dw^2}$$

$$\Rightarrow \boxed{\frac{d^2}{d\lambda^2} = \frac{2H}{ca^3}\frac{d}{dw} + \frac{1}{a^4}\frac{d^2}{dw^2}} \tag{2.116}$$

Substituting these equations (2.115),(2.116) into (2.107) yields:

$$\boxed{\frac{1}{a^4}\frac{d^2\vec{\xi}}{dw^2} + \frac{2H}{ca^3}\frac{d\vec{\xi}}{dw} + \frac{3}{2}\left(\frac{H_0}{c}\right)^2\frac{\Omega_0}{a^5}\vec{\xi} = 0} \tag{2.117}$$

However, since the Universe is expanding we wish to find the propagation equation for the comoving separation vector: $\vec{x} = \frac{1}{a}\vec{\xi}$. Thus, let us start by calculating the derivatives:

$$\frac{d\vec{\xi}}{dw} = \frac{d}{dw}(a\vec{x}) = \frac{da}{dw}\vec{x} + a\frac{d\vec{x}}{dw} = \frac{da}{d\lambda}\frac{d\lambda}{dw}\vec{x} + a\frac{d\vec{x}}{dw}$$

$$\Rightarrow \frac{d\vec{\xi}}{dw} = -\frac{H}{c}a^2\vec{x} + a\frac{d\vec{x}}{dw} \tag{2.118}$$

The second derivative is calculates as follows.

$$\frac{d^2\vec{\xi}}{dw^2} = \frac{d}{dw}\left[-\frac{H}{c}a^2\vec{x} + a\frac{d\vec{x}}{dw}\right] = -\left[\frac{dH}{dw}a^2 + H\frac{d(a^2)}{dw}\vec{x} + Ha^2\frac{d\vec{x}}{dw}\right] + \frac{da}{dw}\frac{d\vec{x}}{dw} + a\frac{d^2\vec{x}}{dw^2} \tag{2.119}$$

We start by calculating the dH/dw term separately:

$$\frac{dH}{dw} = \frac{d}{dw}\left(\frac{1}{a}\frac{da}{dt}\right)$$

$$\Rightarrow \frac{dH}{dw} = \frac{aH^2}{c} - \frac{\ddot{a}}{c} \tag{2.120}$$

Calculating the rest of the terms in a similar way, we eventually obtain:

$$\frac{d^2\vec{\xi}}{dw^2} = a\frac{d^2\vec{x}}{dw^2} - \frac{2a^2H}{c}\frac{d\vec{x}}{dw} + \left[\frac{a^3H^2}{c^2} - \frac{\ddot{a}a^2}{c^2}\right] \tag{2.121}$$

Substituting equations (2.120) and (2.121) into (2.117) and doing the necessary algebra we obtain:

$$\boxed{\frac{d^2\vec{x}}{dw^2} + \left[-\frac{a^2H^2}{c^2} + \frac{\ddot{a}a}{c^2} + \frac{3}{2}\frac{H_0^2}{c^2}\frac{a^3\Omega_0}{a^4}\right]\vec{x}} \tag{2.122}$$

which does not include firt-order derivatives with respect to time, as it should be. This is the propagation equation and it can be significantly simplified further by substituting H^2 and $\ddot{a}$ from Friedman equations which are given by:

$$\frac{\ddot{a}}{a} = -\frac{4\pi G}{3}\rho + \frac{\Lambda}{3} = -\frac{1}{2}\frac{H_0^2\Omega_0}{a^3} + H_0^2\Omega_\Lambda \tag{2.123}$$

$$H^2 = H_0^2\left(\frac{\Omega_0}{a^3} + \Omega_\Lambda - \frac{Kc^2}{a^2H_0^2}\right) \tag{2.124}$$

Substituting these equations into the propagation equation yields:

$$\frac{d^2\vec{x}}{dw^2} + \frac{H_0^2}{c^2}\left[-a^2\left(\frac{\Omega_0}{a^3} + \Omega_\Lambda - \frac{Kc^2}{a^2H_0^2}\right) + a^2\left(-\frac{1}{2}\frac{H_0^2\Omega_0}{a^3} + \Omega_\Lambda\right) + \frac{3}{2}\frac{\Omega_0}{a}\right]\vec{x} = 0$$

$$\Rightarrow \frac{d^2\vec{x}}{dw^2} + \frac{H_0^2}{c^2}\left[-\frac{\Omega_0}{a} - a^2\Omega_\Lambda + \frac{Kc^2}{H_0^2} - \frac{1}{2}\frac{\Omega_0}{a} + a^2\Omega_\Lambda + \frac{3}{2}\frac{\Omega_0}{a}\right]\vec{x} = 0$$

$$\Rightarrow \boxed{\frac{d^2\vec{x}}{dw^2} + K\vec{x} = 0} \tag{2.125}$$

However, we are interested in propagation of light rays through an inhomogeneous Universe and hence we have to include inhomogeneities in the above equation (2.125). We assume that the potential Φ of the inhomogeneities is small compared to the speed of light, implying that inhomogeneities move much slower than light and they are hence localised. Therefore, there exists a local neighbourhood around each density perturbation which is large enough to contain the perturbation completely and small enough to be considered flat. Thus, the metric we consider for the perturbations is actually the perturbed Minkowski metric which we encountered in Section 2.1 and is given by equation (2.13). We've already studied this case and we found that the propagation equation is

given by (2.26) which we also write down here:

$$\boxed{\frac{d^2\vec{x}}{dw^2} = -\frac{2}{c^2}\vec{\nabla}_\perp \Phi} \tag{2.126}$$

Now it's pretty much straightforward to include the inhomogeneities into (2.125), but we must first notice something important. In general, any fiducial ray will be deflected by potential gradients along its way and hence we must consider the difference of the gradients of the potential, $\Delta\left(\vec{\nabla}_\perp \Phi\right)$ between the two light rays. Therefore, for a fiducial light ray starting at the observer O into direction $\vec{\theta} = \vec{0}$ and for a neighbouring light ray starting at the same point into direction $\vec{\theta} \neq \vec{0}$, the comoving separation vector, $\vec{x}\left(\vec{\theta}, w\right)$ will be given by:

$$\boxed{\frac{d^2\vec{x}}{dw^2} + K\vec{x} = -\frac{2}{c^2}\Delta\left\{\vec{\nabla}_\perp \Phi\left[\vec{x}\left(\vec{\theta}, w\right), w\right]\right\}} \tag{2.127}$$

This is the propagation equation for a bundle of light travelling through the Large Scale Structure and it will be our starting point for deriving the formula for the deflection angle and the lensing equation.

2.3.2 Deflection angle and lesning equation

Let us study the deflection of light. To do that, we have to solve the propagation equation (2.127) which can be done by means of a Green's function. We define this Green's function $G(w, w')$ on the interval $[0, w_s]$ where w_s is the comoving distance to the source. This function sould satisfy the following conditions:

1. $G(w, w')$ is continuously differentiable in both intervals $[0, w')$ and $(w', w_s]$ and satisfies the homogeneous differential equation:

$$\frac{d^2 G(w, w')}{dw^2} + KG(w, w') = 0 \tag{2.128}$$

   with boundary conditions $\vec{x}(w = 0) = \vec{0}$ and $\frac{d\vec{x}}{dw}|_{w=0} = \vec{\theta}$.

2. $G(w, w')$ is continuous on $[0, w_s]$.

3. The derivative of $G(w, w')$ with respect to w jumps by 1 on the boundary $w = w'$.

4. As a function of w, $G(w, w')$ satisfies the homogeneous boundary conditions on the solution.

The general solution will be written as:

$$\vec{x} = \vec{x}_{hom} + \int_0^{w_s} dw' G(w, w') f(w') \tag{2.129}$$

where $f(w') = -\frac{2}{c^2}\Delta\left[\vec{\nabla}_\perp \Phi\left(f_K(w')\vec{\theta}, w'\right)\right]$. We start by solving the homogeneous equation with the boundary conditions mentioned in condition (1) above. This is just the equation for the harmonic oscillator and hence the solution is given by:

$$\vec{x}(w) = \vec{A}\cos\left(\sqrt{K}w\right) + \vec{B}\sin\left(\sqrt{K}w\right) \tag{2.130}$$

Applying the boundary conditions we easily find that $\vec{A} = \vec{0}$ and $\vec{B} = \left(1/\sqrt{K}\right)\vec{\theta}$ and hence the solution to the homogeneous equation is,

$$\vec{x}(w) = \frac{\sin\left(\sqrt{K}w\right)}{\sqrt{K}}\vec{\theta} \Rightarrow \boxed{\vec{x}(w) = f_K(w)\vec{\theta}} \tag{2.131}$$

where we used the definition (2.93) for arbitrary K. Therefore, we construct the Green's function as:

$$G(w, w') = \begin{cases} A(w')\cos\left(\sqrt{K}w\right) + B(w')\sin\left(\sqrt{K}w\right) & \text{if } w \in [0, w') \\ C(w')\cos\left(\sqrt{K}w\right) + D(w')\sin\left(\sqrt{K}w\right) & \text{if } w \in (w', w_s] \end{cases} \tag{2.132}$$

Applying condition (4) we get:

$$G(0, w') = 0 \qquad \& \qquad \frac{\partial G}{\partial w}|_{w=0} = 0$$

which yields $A = B = 0$ and hence the Green's function is reduced to:

$$G(w, w') = \begin{cases} 0 & \text{if } w < w' \\ C(w')\cos\left(\sqrt{K}w\right) + D(w')\sin\left(\sqrt{K}w\right) & \text{if } w > w' \end{cases} \tag{2.133}$$

with C and D given by condition (3):

$$G(w, w')|_{w=w'_-} = G(w, w')|_{w=w'_+} \qquad \& \qquad \frac{\partial G}{\partial w}|_{w=w'_+} - \frac{\partial G}{\partial w}|_{w=w'_-} = 1$$

Applying these equations into (2.133) yields a system of two equations with two unknowns:

$$C = -D\frac{\sin\left(\sqrt{K}w'\right)}{\cos\left(\sqrt{K}w'\right)} \qquad \& \qquad -C\sin\left(\sqrt{K}w'\right) + D\cos\left(\sqrt{K}w'\right) = \frac{1}{\sqrt{K}} \tag{2.134}$$

Solving the system is easy and the output is:

$$C = -\frac{1}{\sqrt{K}}\sin\left(\sqrt{K}w'\right) \qquad \& \qquad D = \frac{1}{\sqrt{K}}\cos\left(\sqrt{K}w'\right) \tag{2.135}$$

Putting all the above together, the Green's function we've constructed is:

$$G(w > w', w') = \frac{1}{\sqrt{K}} \left[\cos\left(\sqrt{K}w'\right) \sin\left(\sqrt{K}w\right) - \sin\left(\sqrt{K}w'\right) \cos\left(\sqrt{K}w\right) \right] \tag{2.136}$$

Using the trigonometric identity: $\sin(x \pm y) = \sin(x)\cos(y) \pm \cos(x)\sin(y)$ we can rewrite (2.136) as:

$$G(w > w', w') = \frac{1}{\sqrt{K}} \sin\left[\sqrt{K}\left(w - w'\right)\right] = f_K(w - w') \tag{2.137}$$

Thus, the Green's function that solves the propagation equation is:

$$\boxed{G(w, w') = \begin{cases} f_K(w - w') & \text{if } w > w' \\ 0 & \text{if } w < w' \end{cases}} \tag{2.138}$$

and the solution to the equation according to (2.129) is,:

$$\boxed{\vec{x} = f_K(w)\vec{\theta} - \frac{2}{c^2} \int_0^{w_s} dw' f_K(w - w') \vec{\nabla}_\perp \Phi} \tag{2.139}$$

The deflection angle is then defined as the deviation between the perturbed and the unperturbed path:

$$\boxed{\vec{\alpha} = \frac{f_K(w)\vec{\theta} - \vec{x}}{f_K(w)} = \frac{2}{c^2} \int_0^{w_s} dw' \frac{f_K(w - w')}{f_K(w)} \vec{\nabla}_\perp \Phi[f_K(w')\vec{\theta}, w']} \tag{2.140}$$

which is actually the lensing equation written in a different way. Let us compare this equation with the one we had for a static spacetime in (2.30). We see that they are pretty much he same, with the only difference being that distances in (2.140) are promoted to comoving distances because of the expanding spacetime. We could have derived equation (2.140) heuristically and avoiding all the intervening tedious algebra by just stating that the lensing equation in an expanding spacetime should be the same with the one in a static spacetime with the only change being that distances are now comoving.

2.3.3 Effective Convergence and Shear Correlation Functions

The deflection angle is a basic quantity and once we know it, we can derive further important quantities for lensing, such as the convergence. Notice here, that since we are going after lensing in an expanding homogeneous spacetime, convergence is substituted by the so-called *effective convergence*, κ_{eff}. We know that convergence is half the Laplacian of the lensing potential. Using (2.36), we can relate convergence to the deflection angle by:

$$\kappa_{eff}(\vec{\theta}, w) = \frac{1}{2} \vec{\nabla}_{\vec{\theta}} \vec{\alpha}(\vec{\theta}, w) \tag{2.141}$$

The expressions we derived though, contain the gradient with respect to the transverse components and not θ. This can be fixed by noticing that:

$$\vec{\nabla}_{\perp}\Phi = \frac{1}{f_K(w)}\vec{\nabla}_{\vec{\theta}}\Phi \tag{2.142}$$

Using the formula for the deflection angle we derived above, (2.140) we find for the convergence:

$$\kappa_{eff} = \frac{1}{2}\frac{2}{c^2}\int_0^{w_s} dw' \frac{f_K(w')f_K(w-w')}{f_K(w)}\vec{\nabla}_{\perp}\cdot\vec{\nabla}_{\perp}\Phi\left[f_K(w')\vec{\theta'}, w'\right]$$

$$\Rightarrow \kappa_{eff} = \frac{1}{c^2}\int_0^{w_s} dw' \frac{f_K(w')f_K(w-w')}{f_K(w)}\vec{\nabla}^2_{\perp}\Phi\left[f_K(w')\vec{\theta'}, w'\right] \tag{2.143}$$

We've already emphasized that convergence's power spectrum is related to the matter power spectrum. Let us finally prove this. We can safely assume that $\partial\Phi/\partial z = 0$ and hence $\vec{\nabla}_{\perp}$ can be substituted by $\vec{\nabla}$ at the boundaries of the perturbations. This way, we can exploit the Poison equation,

$$\vec{\nabla}^2\Phi = 4\pi G\rho \tag{2.144}$$

Including density perturbations, the full Poisson equation including both background and perturbations is written as:

$$\vec{\nabla}^2\Phi = 4\pi G\bar{\rho}_0 a^{-1}\left(1+\delta\right) \tag{2.145}$$

where δ is the density contrast $\delta = \delta\rho/\bar{\rho}_0$, with $\delta\rho$ being the density perturbation. Restricting only to the perturbation part of the Poisson equation-which is what we are interested in- yields:

$$\vec{\nabla}^2\Phi = \frac{4\pi G}{a}\bar{\rho}_0\delta \tag{2.146}$$

Using the density parameter which is what cosmological surveys measure, the above equation is written as:

$$\boxed{\vec{\nabla}^2\Phi = \frac{3}{2}H_0^2\Omega_0\frac{\delta}{a}} \tag{2.147}$$

Plugging (2.147) into the equation for convergence (2.143) yields:

$$\boxed{\kappa_{eff} = \frac{3\Omega_0}{2}\left(\frac{H_0}{c}\right)^2\int_0^{w_s} dw' \frac{f_K(w')f_K(w-w')}{f_K(w)}\frac{\delta\left[f_K(w')\vec{\theta'}, w'\right]}{a}} \tag{2.148}$$

Let's take a moment and look carefully at the equation we just derived. The rhs of the equation

is full of cosmology information. It contains Ω_0, H_0, comoving distances that depend on the cosmological model and of course the density contrast which is related to the LSS. The matter power spectrum measured by LSS is defined as:

$$\mathscr{P}_\delta = |\hat{\delta}(\vec{k})|^2 \tag{2.149}$$

It is hence now obvious from (2.148), how convergence can constrain cosmology. Let us proceed by deriving the exact relation between the power spectra of convergence and matter, a task that requires some algebraic work.

If the sources are distributed in redshift, or equivalently in coordinate distance w, the mean effective convergence up to a distance w_H is:

$$\langle\kappa_{eff}\rangle(\vec{\theta}) = \int_0^{w_H} dw G(w)\kappa_{eff}(\vec{\theta}, w) \tag{2.150}$$

where $G(w)$ is the probability to find a source within dw of w. Using the expression we derived for the convergence (2.148), we can write the latter equation as:

$$\langle\kappa_{eff}\rangle(\vec{\theta}) = \frac{3H_0^2\Omega_0}{2c^2}\int_0^{w_H} W(w)f_K(w)\frac{\delta\left[f_K(w)\vec{\theta}, w\right]}{a(w)} \tag{2.151}$$

where we defined the effective weight function by:

$$W(w) = \int_w^{w_H} G(w')\frac{f_K(w'-w)}{f_K(w')} \tag{2.152}$$

It is impossible to predict exactly which density fluctuation caused the deflection on the trajectory of a light ray and we hence need a statistical approach to compute the effective convergence. This statistical measure is the 2-point correlation function, *i.e.* the function that tells us what is the correlation between the convergence at $\vec{\theta}$ and at $\vec{\theta}+\vec{\phi}$. So, we want to compute the following function:

$$\xi_\kappa(\vec{\phi}) = \langle\kappa(\vec{\theta})\kappa(\vec{\theta}+\vec{\phi})\rangle_{\vec{\theta}} \tag{2.153}$$

in which the average extends over all positions $\vec{\theta}$ on the sky and over all directions of the separation vector $\vec{\phi}$. Due to isotropy, the result won't depend on the direction of $\vec{\phi}$ and hence $\xi_\kappa(\vec{\phi}) = \xi_\kappa(\phi)$. It is more convenient to perform the calculations in Fourier space. Let us first demonstrate how correlation functions work by considering a general case and then we'll apply it on convergence. Suppose we have a function $g(x)$ whose correlation is given by:

$$\xi_{gg}(y) = \langle g(x)g(x+y)\rangle_x \tag{2.154}$$

Defining the Fourier transform and its inverse:

$$\hat{g}(k) = \int d^n x g(x) e^{ik\cdot x} \qquad , \qquad g(x) = \int \frac{d^n k}{(2\pi)^n} \hat{g}(k) e^{-ik\cdot x} \tag{2.155}$$

Thus, the correlation function in Fourier space is given by:

$$\hat{\xi}_{gg}(k) = \langle \hat{g}(k) \hat{g}^*(k') \rangle \tag{2.156}$$

$$\Rightarrow \hat{\xi}_{gg}(k) = \left\langle \int d^n x g(x) \int d^n x' g(x') e^{ik\cdot x} e^{-ik'\cdot x'} \right\rangle$$

$$\Rightarrow \hat{\xi}_{gg}(k) = \left\langle \int d^n x e^{ik\cdot x} \int d^n x' g(x') g(x) e^{-ik'\cdot x'} \right\rangle$$

Performing a change of variables: $x' = x + y$ yields:

$$\hat{\xi}_{gg}(k) = \int d^n x e^{ik\cdot x} \int d^n y e^{-ik'\cdot x} e^{-ik'\cdot y} \langle g(x) g(x+y) \rangle$$

$$\Rightarrow \hat{\xi}_{gg}(k) = \int d^n x e^{i(k-k')x} \int d^n y e^{-ik'\cdot y} \xi_{gg}(y)$$

$$\Rightarrow \hat{\xi}_{gg}(k) = (2\pi)^n \, \delta_D^n(k-k') \int d^n y e^{-ik'\cdot y} \xi_{gg}(y)$$

where we used the property of the Dirac delta function:

$$\int d^n x e^{i(k-k')x} = (2\pi)^n \, \delta_D^n(k-k') \tag{2.157}$$

We also define the power spectrum of the function g by:

$$\mathscr{P}_g(k) = \int d^n y e^{-ik\cdot y} \xi_{gg}(y) \tag{2.158}$$

and hence the correlation function of g is given by:

$$\boxed{\hat{\xi}_{gg}(k) = (2\pi)^n \, \delta_D^n(k-k') \mathscr{P}_g(k')} \tag{2.159}$$

which means that the Fourier transform of the correlation function is the power spectrum and

vice-versa.

Let us now assume that we are given the power spectrum of a three-dimensional function $\delta(\vec{x})$ and we want to find its two-dimensional projection:

$$g(\vec{\theta}) = \int dw q(w) \delta[f_K(w)\vec{\theta}, w] \tag{2.160}$$

where $q(w)$ is the weight function. We start from the correlation function of g which according to what we showed above is given by:

$$\xi_{gg} = \int dw q(w) \int dw' q(w') \Big\langle \delta[f_K(w)\vec{\theta}, w]\delta[f_K(w')\vec{\theta'}, w'] \Big\rangle \tag{2.161}$$

Inserting the Fourier transform of the function δ yields:

$$\xi_{gg} = \int dw q(w) \int dw' q(w') \Big\langle \int \frac{d^3k}{(2\pi)^3} e^{-i\vec{k}\cdot\vec{\theta}} \hat{\delta}(\vec{k}) \int \frac{d^3k'}{(2\pi)^3} e^{i\vec{k'}\cdot\vec{\theta'}} \hat{\delta}^*(\vec{k'}) \Big\rangle$$

$$\Rightarrow \xi_{gg} = \int dw \int dw' \int \frac{d^3k}{(2\pi)^3} \int \frac{d^3k'}{(2\pi)^3} \langle \hat{\delta}(\vec{k})\hat{\delta}^*(\vec{k'})\rangle e^{-i\vec{k}\cdot\vec{\theta}} e^{i\vec{k'}\cdot\vec{\theta'}} \tag{2.162}$$

Let us split the vector $\vec{k}$ into a perpendicular part, $\vec{k}_\perp$, and a parallel part k_s. The exponential will then become:

$$e^{-i\vec{k}\cdot\vec{\theta}} = \exp\Big[-if_K(w)\vec{\theta}\cdot\vec{k}_\perp - ik_s w\Big] = e^{-if_k(w)\vec{\theta}\cdot\vec{k}_\perp} e^{-ik_s w} \tag{2.163}$$

$$e^{i\vec{k'}\cdot\vec{\theta'}} = \exp\Big[if_K(w')\vec{\theta'}\cdot\vec{k'}_\perp + ik'_s w'\Big] = e^{if_k(w')\vec{\theta'}\cdot\vec{k'}_\perp} e^{ik'_s w'} \tag{2.164}$$

Plugging equations (2.163), (2.164) in (2.162) and using the definition of power spectrum (2.159) yields:

$$\xi_{gg} = \int dw q^2(w) \int \frac{d^3k}{(2\pi)^3} \mathscr{P}_\delta(\vec{k}, w) \exp\Big[-if_K(w)\vec{k}_\perp \cdot \Big(\vec{\theta} - \vec{\theta'}\Big)\Big] e^{-ik_s w} \int dw' e^{ik_s w'}$$

where the delta function set $\vec{k} = \vec{k'}$. Using again the delta function property:

$$\xi_{gg} = \int dw q^2(w) \int \frac{d^3k}{(2\pi)^3} \mathscr{P}_\delta(\vec{k}, w) \exp\Big[-if_K(w)\vec{k}_\perp \cdot \Big(\vec{\theta} - \vec{\theta'}\Big)\Big] e^{-ik_s w} 2\pi\delta_D(k_s) \tag{2.165}$$

The delta function cancels the integration with respect to k_s, implying that the only contribution to the correlation function comes from the modes perpendicular to the line of sight. Therefore,

$$\xi_{gg} = \int dw q^2(w) \int \frac{d^2\vec{k}_\perp}{(2\pi)^2} \mathscr{P}_\delta(|\vec{k}_\perp|) e^{if_K(w)(\vec{\theta}-\vec{\theta'})\cdot\vec{k}_\perp}$$

Defining the separation by $\vec{\phi} = \vec{\theta} - \vec{\theta'}$ and using isotropy we obtain:

$$\boxed{\xi_{gg}(\phi) = \int dw q^2(w) \int \frac{d^2\vec{k}_\perp}{(2\pi)^2} \mathscr{P}_\delta(|\vec{k}_\perp|) e^{-i f_K(w)\vec{k}_\perp \cdot \vec{\phi}}} \tag{2.166}$$

Now that we have the correlation function, we can calculate the power spectrum of the projection g, which according to (2.158) is given by:

$$\mathscr{P}_g = \int d^2\phi e^{i\vec{l}\cdot\vec{\phi}} \xi_{gg}(\phi) \tag{2.167}$$

Plugging in the expression for the correlation function (2.166) yields:

$$\mathscr{P}_g(l) = \int dw q^2(w) \int \frac{d^2\vec{k}_\perp}{(2\pi)^2} e^{i\vec{l}\cdot\vec{\phi}} \mathscr{P}_\delta(\vec{k}_\perp, w) e^{-i f_K(w)\vec{k}_\perp \cdot \vec{\phi}}$$

$$\Rightarrow \mathscr{P}_g(l) = \int dw q^2(w) \int \frac{d^2\vec{k}_\perp}{(2\pi)^2} \mathscr{P}_\delta(\vec{k}_\perp, w) e^{i\vec{\phi}\cdot[\vec{l} - f_K(w)\vec{k}_\perp]}$$

$$\Rightarrow\Rightarrow \mathscr{P}_g(l) = \int dw q^2(w) \int \frac{d^2\vec{k}_\perp}{(2\pi)^2} \mathscr{P}_\delta(\vec{k}_\perp, w) (2\pi)^2 \delta_d^{(2)}\left(\vec{l} - f_K(w)\vec{k}_\perp\right)$$

The delta function "kills" the integral and sets $\vec{k}_\perp = \vec{l}/f_K(w)$ and hence the latter expression reduces to:

$$\boxed{\mathscr{P}_g(l) = \int dw q^2(w) \frac{1}{f_k^2(w)} \mathscr{P}_\delta\left(\frac{l}{fkw}, w\right)} \tag{2.168}$$

The equation we just derived gives the Power Spectrum of the two-dimensional projection g of the three-dimensional function δ. Let us hence specialize this result to the convergence. Comparing equations (2.168) and (2.151) we deduce that $q(w)$ is given by:

$$q(w) = \frac{3H_0^2\Omega_0}{2c^2} W(w) \frac{f_K(w)}{a(w)} \tag{2.169}$$

and plugging this into (2.168) where we set $g = \kappa$ yields:

$$\boxed{\mathscr{P}_\kappa(l) = \frac{9H_0^4\Omega_0^2}{4c^4} \int_0^{w_H} dw \frac{W^2(w)}{a^2(w)} \mathscr{P}_\delta\left(\frac{l}{f_K(w)}, w\right)} \tag{2.170}$$

where the $W(w)$ function is an expression of the comoving distances. This equation makes clear the connection between weak lensing and cosmology and we will come back to it in the next section 2.4

Observations however, do not measure convergence. They give a measurement of galaxy ellipticity which is actually an estimator for shear, because for $\kappa \ll 1$, we can perform a Taylor expansion in equation (2.55) and prove that $\epsilon = \gamma$. Recall that convergence and shear have the same power spectrum and hence to make the connection to cosmology, we need to calculate first the shear power spectrum, or the shear correlation function.

- **Shear Correlation Functions**

We consider a pair of galaxies at $\vec{\theta}$ separated by $\vec{\phi}$. We can use the polar angle φ of the separation vector $\vec{\phi}$ to define the tangential and cross components of shear by:

$$\gamma_t = \gamma \cos(2\varphi) \qquad \& \qquad \gamma_\times = \gamma \sin(2\varphi) \tag{2.171}$$

Using these two shear components, we can define the following three combinations of correlation functions:

$$\xi_{tt}(\phi) = \left\langle \gamma_t(\vec{\theta})\gamma_t(\vec{\theta}+\vec{\phi}) \right\rangle \tag{2.172}$$

$$\xi_{\times\times}(\phi) = \left\langle \gamma_\times(\vec{\theta})\gamma_\times(\vec{\theta}+\vec{\phi}) \right\rangle \tag{2.173}$$

$$\xi_{t\times}(\phi) = \left\langle \gamma_t(\vec{\theta})\gamma_\times(\vec{\theta}+\vec{\phi}) \right\rangle \tag{2.174}$$

Let us begin by the tangential correlation function which can be written as the inverse Fourier transform of the tangential shear power spectrum:

$$\xi_{tt}(\phi) = \int \frac{d^2l}{(2\pi)^2} \mathscr{P}_{\gamma_t}(l) e^{-i\vec{l}\cdot\vec{\phi}} \tag{2.175}$$

where the tangential shear power spectrum is:

$$\mathscr{P}_{\gamma_t}(l) = \langle \hat{\gamma}_t(l)\hat{\gamma}_t{}^*(l) \rangle = \frac{l^4}{4} \left(\cos^2(\varphi) - \sin^2(\varphi) \right) \mathscr{P}_\psi(l) \tag{2.176}$$

where $\mathscr{P}_\psi(l)$ is the power spectrum of the lensing potential. Using equation (2.77) and the definition of the power spectrum, the above equation becomes:

$$\mathscr{P}_{\gamma_t}(l) = \left(\cos^2(\varphi) - \sin^2(\varphi) \right) \mathscr{P}_\kappa(l) \tag{2.177}$$

Plugging the latter equation into the expression for the correlation function (2.175) yields:

$$\xi_{tt}(\phi) = \frac{d^2l}{(2\pi)^2} \left(\cos^2(\varphi) - \sin^2(\varphi) \right) e^{-i\vec{l}\cdot\vec{\phi}} \mathscr{P}_\kappa(l)$$

Carrying out the integration with respect to the polar angle gives a factor of 2π and hence the integral reduces to:

$$\boxed{\xi_{tt}(\phi) = \int \frac{ldl}{2\pi} \mathscr{P}_\kappa(l) \left[\mathscr{J}_0(l\phi) + \mathscr{J}_4(l\phi) \right]} \tag{2.178}$$

where $\mathscr{J}(l\phi)$ are the Bessel functions of the first kind defined as:

$$\mathscr{J}_n(x) = \frac{(-i)^n}{\pi} \int_0^\pi dm e^{ixm} \cos(nm) \tag{2.179}$$

Repeating the exact same process for the cross shear, we can easily find that the cross correlation function is given by:

$$\boxed{\xi_{\times\times}(\phi) = \int \frac{ldl}{2\pi} \mathscr{P}_\kappa(l) \left[\mathscr{J}_0(l\phi) - \mathscr{J}_4(l\phi) \right]} \tag{2.180}$$

For the mixed correlation function, $\xi_{t\times}(\phi) = \xi_{\times t}(\phi) = 0$, which provides a test of reliability, since a non-zero value points to systematics. Taking these into account, we can define the following combinations:

$$\boxed{\xi_\pm(\phi) = \langle \gamma_t \gamma_t' \rangle \pm \langle \gamma_\times \gamma_\times' \rangle} \tag{2.181}$$

where the prime denotes that the shear component is evaluated at the separation point. Using equations (2.172), (2.173), (2.178) and (2.180) we can write $\xi_+(\phi)$ and $\xi_-(\phi)$ as:

$$\xi_+(\phi) = \int \frac{ldl}{2\pi} \mathscr{P}_\kappa(l) \mathscr{J}_0(l\phi) \qquad , \qquad \xi_-(\phi) = \int \frac{ldl}{2\pi} \mathscr{P}_\kappa(l) \mathscr{J}_4(l\phi) \tag{2.182}$$

Thus, to obtain the convergence spectrum, we use the orthonormality of Bessel functions to write:

$$\boxed{\mathscr{P}_\kappa(l) = 2\pi \int_0^\infty d\phi\phi\xi_+(\phi) \mathscr{J}_0(l\phi) = 2\pi \int_0^\infty d\phi\phi\xi_-(\phi) \mathscr{J}_4(l\phi)} \tag{2.183}$$

But how do we actually measure the shear correlation functions? As we've stated before, the estimator for measuring shear is the galaxy's observed ellipticity. Therefore, the estimator for computing the shear correlation functions is:

$$\boxed{\xi_\pm(\phi) = \langle \epsilon_t \epsilon_t' \rangle \pm \langle \epsilon_\times \epsilon_\times' \rangle} \tag{2.184}$$

where we know that ellipticity is measured from the surface brightness distribution using the quadrupole moments as described in Section 2.2.

2.4 Connection to Cosmology

It is now time to make the connection between cosmology and weak lensing. The process goes like this:

1. Measure galaxy ellipticity via the surface brightness distribution using the quadrupole moments as described in equations (2.67), (2.68).

2. Use this result and plug it into the estimator for shear correlation functions (2.184).

3. Once $\xi_+(\phi)$ and $\xi_-(\phi)$ are computed, plug the result into (2.183) to obtain the convergence power spectrum.

4. Finally, use the convergence power spectrum to constrain cosmology via equation (2.170).

Cosmological parameters are measured by using Bayesian statistics[7]. Assuming that correlation functions have been measured in n bins, these measurements define the data vector $\vec{\xi}_{obs}$. We can then define the likelihood of the data given a set of cosmological parameters $\vec{p}$ as $\mathscr{L}\left(\vec{\xi}_{obs}|\vec{p}\right)$. Assuming that the likelihood is Gaussian in the parameter space, it can be written as (see [1]):

$$\mathscr{L}\left(\vec{\xi}_{obs}|\vec{p}\right) = \frac{1}{(2\pi)^n\,|\vec{S}|}\exp\left[-\frac{1}{2}\left(\vec{\xi}_{obs}-\vec{\xi}_{model}\right)^T\vec{S}^{-1}\left(\vec{\xi}_{obs}-\vec{\xi}_{model}\right)\right] \tag{2.185}$$

where $\vec{\xi}_{model}$ describes the theoretical predictions for the shear correlations computed for the same angular bins with the fiducial cosmological model characterized by the parameters $\vec{p}$ and $\vec{S}$ is the covariance matrix defined as:

$$\vec{S} = \left\langle \left(\vec{\xi}_{obs}-\vec{\xi}_{model}\right)^T\left(\vec{\xi}_{obs}-\vec{\xi}_{model}\right)\right\rangle \tag{2.186}$$

where the average is over many realisations of the survey under consideration. To determine the parameters we use Bayes theorem, according to which the posterior is given by:

$$\mathscr{P}(\vec{p}|\vec{\xi}_{obs}) \propto \mathscr{L}\left(\vec{\xi}_{obs}|\vec{p}\right)\mathscr{P}(\vec{p}) \tag{2.187}$$

where $\mathscr{P}(\vec{p})$ is the prior probability. The parameters are then constrained by maximizing the likelihood.

[7]For a comprehensive analysis of this subject, check [50]

3 Galaxy Light Polarization and Weak Lensing

We have thus far discussed in depth cosmic shear as a probe for cosmology and we have also emphasized in Section 1.3 that weak lensing is a very noisy effect. It is already mentioned that the goal of this project is to alleviate some of the shape noise in WL measurements by means of combining galaxy's polarisation and cosmic shear. In this chapter, we enter the research phase of this project. We start by discussing in brief the concept of polarisation and we quantify this phenomenon by introducing the Stokes parameters and the degree of polarisation. Afterwards, we mention theoretical models predicting the orientation of the degree of polarisation and we then make the connection to WL by constructing an optimal estimator for shear, including polarisation. Finally, we put this estimator at work by means of numerical simulations.

3.1 Concept of Polarisation

Astronomy involves the reception of light from distant objects, beyond Earth. This light is nothing else but electromagnetic radiation, *i.e.* an electromagnetic wave propagating in space. For the electric field vector, we consider a monochromatic light ray travelling along the $+\hat{z}$-axis with the propagation equation given by:

$$\vec{E}(z,t) = \vec{E}_0 e^{i(2\pi\nu t - kz)} = (E_x\hat{x} + E_y\hat{y})\, e^{i(2\pi\nu t - kz)} \tag{3.1}$$

where k is the wavenumber and ν is the frequency of the wave, E_x and E_y are the components of the electric field vector. This equation is a solution to Maxwell's equation in vacuum and describes the polarised propagation of an electromagnetic wave along the $\hat{z}$-axis. Notice that we used a Cartesian coordinate system. However, when it comes to polarisation people use more often a different coordinate system describing left-hand and right-hand circular polarisations (LCP and RCP). This system is defined by:

$$\hat{R} = \frac{1}{\sqrt{2}}(\hat{x} - i\hat{y}) \qquad \& \qquad \hat{L} = \frac{1}{\sqrt{2}}(\hat{x} + i\hat{y}) \tag{3.2}$$

In this new basis, equation (3.1) may be rewritten as:

$$\vec{E}(z,t) = \vec{E}_0 e^{i(2\pi\nu t - kz)} = \left(E_R\hat{R} + E_L\hat{L}\right) e^{i(2\pi\nu t - kz)} \tag{3.3}$$

Polarisation is a central quantity in radio astronomy (see [51] for a comprehensive review). Radio signals are, in general, partially polarised and to describe this polarisation, we need to define some parameters. The parameters used more often are the *Stokes* parameters denoted by I, Q, U, V and given by:

$$I \equiv I_{total} \equiv I_{0^\circ} + I_{90^\circ} \equiv I_{45^\circ} + I_{-45^\circ} \tag{3.4}$$

$$Q \equiv I_{0^\circ} - I_{90^\circ} \tag{3.5}$$

$$U \equiv I_{45^\circ} - I_{-45^\circ} \tag{3.6}$$

$$V \equiv I_{RCP} - I_{LCP} \tag{3.7}$$

Let us now explain the meaning of each parameter.

- I is the total intensity and it is he sum of any two orthogonal polarisation components, and it hence does not store any polarisation information.

- Q is the difference in intensities between the horizontal and vertical linearly polarised components and is a measure of the tendency of the radio wave to prefer the horizontal direction. So, if $Q > 0$, there is an excess of polarized radiation along the horizontal and if $Q < 0$, there is a vertical excess.

- U is the difference in intensities between linearly polarised components at $+45^\circ$ and -45° and represents the preference of the light to be aligned at $+45^\circ$.

- V is the difference between the intensities of the RCP and LCP components and describes the preference for the light to be RCP.

The most important quantity for our research is the degree of polarisation, which is defined as the ratio of the intensity of the polarized emission to the total intensity :

$$p = \frac{I_{pol}}{I_{tot}} = \frac{\sqrt{Q^2 + U^2 + V^2}}{I} \tag{3.8}$$

with p of course being $0 \leq p \geq 1$. We can also define the linear fraction as:

$$p_{lin} = \frac{\sqrt{Q^2 + U^2}}{I} \tag{3.9}$$

with $0 \leq p_{lin} \geq 1$.
The most important property of the degree of polarisation (hereafter, polarisation) is that it is a spin-2 quantity, just as shear and ellipticity.

Now that we've defined all the quantities we need to describe polarisation, let us focus on the optical light emitted from distant disk galaxies. This light contains a mixture of information about the stellar distribution and the dust. Besides extinction, dust scatters light and this can have an important effect on the galaxy's appearance. One of the manifestations of this scattering is polarisation. Theoretical models studying this phenomenon, have provided us with some predictions about the direction of polarisation. Wood *et. al* [52] studied the pattern to be expected from scattering by dust in simple-double exponential disks at various inclinations and found that the maximum degree of linear polarisation is 2% as it is shown in the following figure 15:

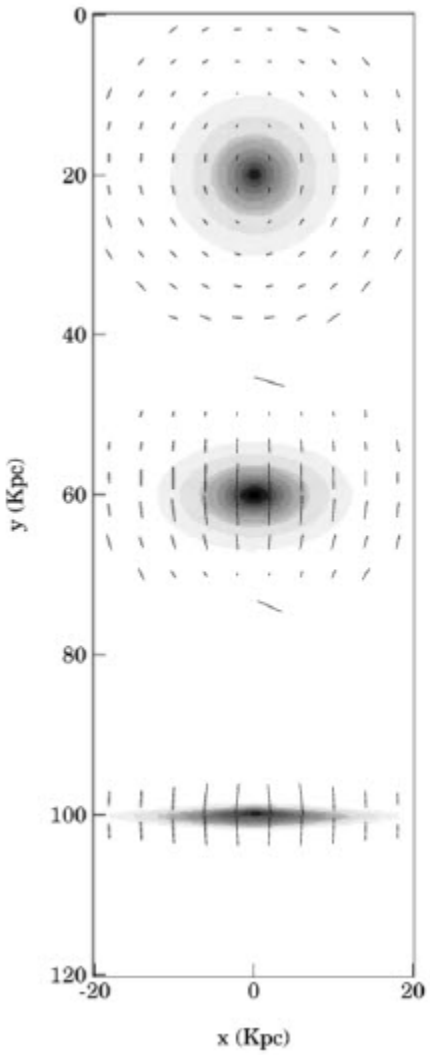

Figure 15: Models for the polarisation of starlight after being scattered by dust distributed among the stars in the stellar disk [52]. The longest bars correspond to 2% polarisation.

There also exist more complex models that include dichroic absorption by dust that tend to have somewhat lower overall polarisation. However, it is clear that the models predict a clear alignment of the overall polarisation of inclined disk galaxies with their minor axis [45, 46, 53, 54]. We thus

realise that the direction of polarization can possibly carry information on the intrinsic ellipticity of the galaxy, since it is not affected by lensing (see figure 7). Thus, our next step is to combine polarisation and weak lensing.

3.2 Combining Polarisation and Weak Lensing

We wish to construct an estimator for measuring shear which will include polarisation. The usual estimator we have for shear is averaging the observed ellipticity:

$$\Gamma_{usual} = \epsilon_{obs} \Rightarrow \langle \Gamma_{usual} \rangle = \langle \epsilon_{obs} \rangle = \gamma \tag{3.10}$$

Let us investigate now how to incorporate polarisation. Before constructing the estimator, recall that the whole idea of the project is that polarisation could be correlated to the intrinsic ellipticity of the galaxy. Therefore, we can assume a linear correlation between those two given by:

$$\boxed{p = P\epsilon_{int} + n_p} \tag{3.11}$$

where P is a parameter and n_p is a random noise that depends on the dispersion σ_p. This equation is bound to the following conditions:

- Polarisation on average is zero: $\langle p \rangle = 0$
- since the average of polarisation is zero, its variance is equal to the average of the square of polarisation: $\langle p^2 \rangle = \langle n_p^2 \rangle = \sigma_p^2$.
- According to the intrinsic way that the sky works, galaxies are randomly oriented and their shapes are uncorrelated, meaning that intrinsic ellipticity on average should be zero: $\langle \epsilon_{int} \rangle = 0$
- Since the average of intrinsic ellipticity is zero, its variance is equal to the square of the intrinsic ellipticity, which is the shape noise: $\langle \epsilon_{int}^2 \rangle = \sigma_e^2$.

When lensing occurs, the intrinsic ellipticity changes due to the induced shear and becomes the observed ellipticity:

$$\epsilon_{obs} = \epsilon_{int} + \gamma \tag{3.12}$$

Keeping these in mind, let us proceed to the construction of the shear estimator. This estimator should be optimal and include polarisation. An optimal estimator should satisfy the following two conditions:

1. It is unbiased, meaning that its average is equal to the value it measures.

2. It has minimum variance.

Thus, we can try the simplest relation we can imagine, where the optimal estimator is given by:

$$\Gamma_{opt} = \alpha\epsilon_{obs} + \beta p \tag{3.13}$$

where the parameters α and β are fixed by the unbiased and minimum variance conditions. Condition (1) implies that:

$$\langle \Gamma_{opt} \rangle = \gamma$$

$$\Rightarrow \gamma = \alpha\langle \epsilon_{obs} \rangle + \beta\langle p \rangle$$

$$\Rightarrow \gamma = \alpha\gamma \Rightarrow \boxed{\alpha = 1} \tag{3.14}$$

Therefore, the optimal estimator is,:

$$\Gamma_{opt} = \epsilon_{obs} + \beta p \tag{3.15}$$

Applying condition (2) yields an expression for β. We start by calculating the variance of (3.15):

$$Var\left(\Gamma_{opt}\right) = \left\langle \left(\Gamma_{opt} - \gamma\right)^2 \right\rangle$$

$$\Rightarrow Var\left(\Gamma_{opt}\right) = \left\langle \left(\epsilon_{obs} + \beta p - \gamma\right)^2 \right\rangle$$

Substituting ϵ_{obs} by equation (3.12) and polarisation by (3.11) gives:

$$Var\left(\Gamma_{opt}\right) = \left\langle \left(\epsilon_{int} + \gamma + \beta P\epsilon_{int} + \beta n_p - \gamma\right)^2 \right\rangle$$

$$\Rightarrow Var\left(\Gamma_{opt}\right) = \left\langle \left(\epsilon_{int}\left(1 + \beta P\right) + \beta n_p\right)^2 \right\rangle$$

$$\Rightarrow Var\left(\Gamma_{opt}\right) = \left(1 + \beta P\right)^2 \left\langle \epsilon_{int}^2 \right\rangle + \beta^2 \left\langle n_p^2 \right\rangle + 2\beta\left(1 + \beta P\right) \left\langle \epsilon_{int} n_p \right\rangle$$

The last term on the right-hand-side is equal to zero because intrinsic ellipticity and the polarisation noise are not correlated. Therefore, the variance of the optima estimator is given by:

$$\boxed{Var\left(\Gamma_{opt}\right) = \left(1+\beta P\right)^2 \sigma_e^2 + \beta^2 \sigma_p^2} \tag{3.16}$$

For this variance to be minimum, we demand that: $\partial_\beta \left[Var\left(\Gamma_{opt}\right)\right] = 0$, which yields:

$$2\left(1+\beta P\right) P\sigma_e^2 + 2\beta\sigma_p^2 = 0$$

Solving for β yields:

$$\boxed{\beta = -\frac{P\sigma_e^2}{\sigma_p^2 + P^2\sigma_e^2}} \tag{3.17}$$

Plugging this into the relation for the optimal estimator we obtain:

$$\boxed{\Gamma_{opt} = \epsilon_{obs} - \frac{P\sigma_e^2}{\sigma_p^2 + P^2\sigma_e^2} p} \tag{3.18}$$

Let us take a moment and explain the equation we just derived. We see that if we take the average, it yields the value for shear since $\langle p \rangle = 0$. What changes is the variance. The variance of the optimal estimator includes polarisation, which can carry extra information if $P \neq 0$. Let us explain how an observation would work. Imagine that you have a catalogue of galaxies for which you have performed weak lensing measurements and hence you have measured the observed ellipticity and the shear. Since polarisation is not affected by lensing, you can study again the same galaxies, but this time the goal is to measure the polarisation. So, in the end you will have measured p, ϵ_{obs} and γ for a sample N of galaxies. The goal of this observation is to see if polarisation is correlated to the intrinsic ellipticity of the galaxies, *i.e.* to infer the values of P and σ_P. Thus, after measuring polarisation and shear for the same sample of galaxies, you can infer the intrinsic ellipticity and combine it with the measurement of polarisation in (3.11). Then, equation (3.11) is an equation for which p and ϵ_{int} are known, and the parameters P and σ_p are inferred from the data by a chi-square fitting. If $P \neq 0$, then polarisation is correlated to the intrinsic ellipticity and it can reduce the shape noise of weak lensing measurements. Let us hence put this thought at work, and test if the variance of the optimal estimator is indeed smaller than the one of the usual estimator by means of a "naive" numerical simulation.

3.3 A "naive" numerical simulation

Our goal here is to test if the variance of the optimal estimator is smaller than the variance of the usual one for some values of P and σ_p. This can be tested easily via using Python and the steps are the following:

1. We begin by creating 1000 galaxy catalogues, each galaxy containing 10000 galaxies. We do that by defining each galaxy with a given intrinsic ellipticity. We know for ellipticity that: $0 \leq \epsilon_{int} \leq 1$. Furthermore, it is a spin-2 quantity. We can thus generate a random normal distribution of 10000 ellipticities, with average zero and error σ_e and repeat this process 1000 times. We use $\sigma_e = 0.25$, which is a valid value for galaxies.

2. Do the same thing for the polarisation noise and assume that $\sigma_p = 0.25$ as well. Notice that there is no justification for this value that we chose, since the actual value will be given by the observation. However, our goal here is to just test numerically the variance of the optimal estimator compared to the variance of the usual one.

3. Use equation (3.11) and generate polarisation as a function of the parameter P. Thus, we have created a dataset of ϵ_{int}, n_p and for a given P, a dataset of p.

4. Assume a given shear, say $\gamma = -0.1$.

5. Apply this given shear in equation (3.12) to compute the usual estimator and its variance.

6. Define the optimal estimator according to equation (3.18) as a function of P.

7. Last step: Run the code for different values of P and compare the usual and optimal estimators. If everything is correct, the average of both estimators should be the same, but their variance should be different for non-zero values of P.

Running the code yields indeed $\langle \Gamma_{usual} \rangle = \langle \Gamma_{opt} \rangle = -0.1$ and different variance between those two. The code can be found on the GitHub repository `https://github.com/Chrisostomos-Stamou/Combining-Weak-Lensing-and-Galaxy-Light-Polarisation` in the file titled: "Optimal Estimator.ipynb". We can incorporate all the information from the code into the following plot (figure 16).

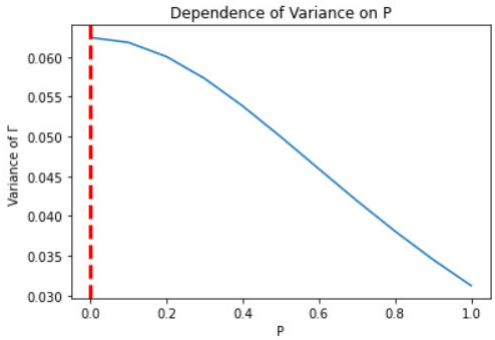

Figure 16: Dependence of the variance of the optimal estimator with respect to different values of P. The red vertical dashed line corresponds to the usual estimator and the blue line to the optimal estimator.

The red dashed line corresponds to $P = 0$, which represents the usual estimator. As P increases, we see that the variance of the optimal estimator decreases. Parameter P defines the "strength" of correlation between polarisation and intrinsic ellipticity as seen from (3.11). Hence, the meaning of this plot is that for a given σ_p, the more correlated polarisation and intrinsic ellipticity are, the less

the variance of the optimal estimator for shear, hence the more the information that polarisation carries for weak lensing measurements.

We deduce that this naive simulation verifies our analytic work. However, in reality cosmic shear is not a single-valued field, but is is an actual field measured by correlation functions. Therefore, to test the effect of polarisation into cosmic shear surveys, we need to consider an actual simulation of a cosmic shear survey and work out the shear correlation functions, which brings us to Chapter 4.

4 Numerical Simulations: using KiDS-450 mock source catalogues

In this chapter, we use the KiDS-450 Mock Source catalogue, provided by the "Scinet Light Cone Simulations" (SLICS). This catalogue includes measurements of shear and observed ellipticity and we can hence put to test the optimal estimator. Our goal is to compare the variance of the optimal estimator and compare it to the variance of the usual estimator. We begin in section 4.1 by repeating the process described in section 3.3 in order to compare the variances, but this time we use the simulated data sets and we don't generate random ones. In section 4.2 we compute the usual shear correlation function by using the code "TreeCorr". We proceed in section 4.3 by constructing the optimal estimator for shear correlation functions by combining equations (3.18) and (2.184). Once this is done, we compute shear correlation functions by using the optimal estimator for different values of P and we compare its variance to the variance of the usual estimator using the observed ellipticity in order to work out which estimator is less noisy. We prove that the more correlated polarisation and intrinsic ellipticity are, the less the variance of the optimal estimator, hence the less the noise.

4.1 Comparison between the estimators

In section 3.3 we tested the variance of the optimal estimator by generating random data sets. Let us now repeat the same process, but this time, we can use the simulated data sets provided by SLICS (`https://slics.roe.ac.uk/`). The calculation is given on the GitHub repository `https://github.com/Chrisostomos-Stamou/Combining-Weak-Lensing-and-Galaxy-Light-Polarisation` in the file titled: "MOCK.ipynb". SLICS is a simulation project that gives a 10×10 degree patch of the sky with galaxies that have been sheared by a cosmological distribution of dark matter and it is given in fits format. We are interested in using the KiDS-450 Mock Source Catalogue, and we chose to work with the first catalogue, titled "GalCatalogue_LOS1.fits". This catalogue contains about three million data points and the output of the catalogue is organised as shown in figure 17.

```
FITS_rec([(151.62956  ,  23.877169, 7.2777580e-04, 0.2149156 ,  2.3887389e-06,  1.7337958e-06,  0.07777154,  0.00264687),
          (399.98856  , 242.06535 , 5.7519907e-03, 0.21083285,  9.0160602e-06,  1.3832255e-05,  0.70206827, -0.06426633),
          (488.29962  , 538.22784 , 6.8415557e-03, 0.21324398,  2.9321502e-05, -6.0476112e-05,  0.10993154,  0.03363911),
          ...,
          ( 53.293072 ,  42.934055, 4.6604691e+00, 0.508582  , -1.8608868e-02, -8.6770132e-03,  0.05565798,  0.2157739 ),
          (  5.6541085, 331.15939 , 4.6648049e+00, 0.50393653,  5.1830737e-03, -2.9979378e-02, -0.60660183, -0.20025468),
          (239.81259  , 157.34943 , 4.6659331e+00, 0.508609  ,  5.4329624e-03,  2.7184695e-02, -0.14238249,  0.42247179)],
         dtype=(numpy.record, [('x_arcmin', '>f8'), ('y_arcmin', '>f8'), ('z_spectroscopic', '>f8'), ('z_photometric', '>f
8'), ('shear1', '>f8'), ('shear2', '>f8'), ('eps_obs1', '>f8'), ('eps_obs2', '>f8')]))
```

Figure 17: The output of the KiDS-450 Mock Source catalogue 1.

We see that the first and the second columns give the x and y coordinates respectively in units of *arcmin*. The third and fourth columns correspond to the spectroscopic and photometric redshift respectively, but we won't use them because they are unrelated to our goal. What we will extensively use, is the rest of the columns. The fifth and the sixth columns correspond to γ_1 and γ_2

respectively, while the last two columns correspond to $\epsilon_{obs,1}$ and $\epsilon_{obs,2}$.

The catalogue provides us with the values of observed ellipticity and shear. Therefore, we can derive the intrinsic ellipticity for each point by equation (3.12) and then we can derive the corresponding polarisation, for different values of P and σ_p. This allows us to calculate the usual estimator given by averaging the observed ellipticities and the optimal estimator given by (3.18). Repeating the exact same process as in section 3.3 we obtain the following plot (figure 18):

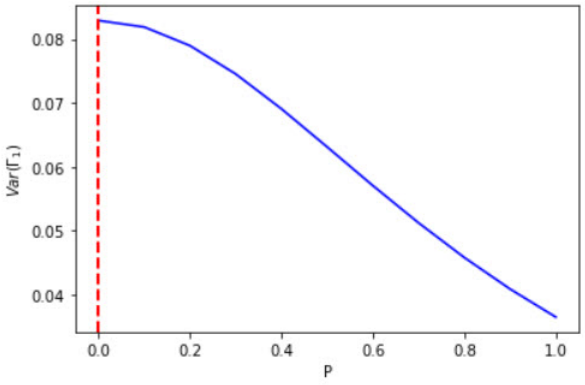

Figure 18: Dependence of the variance of the optimal estimator on the value of P, after choosing $\sigma_p = 0.25$.

We see that we obtain the same result as in figure 17, but this time the values for the variance are different. We should mention here that the estimator is an expression of spin-2 quantities and it is hence a spin-2 quantity as well. Therefore, we are calculating two components Γ_1^{opt} and Γ_2^{opt}. The dependence of the variance on the value of P for both components is exactly the same, so plotting only the Γ_1 component is adequate.

4.2 Usual Estimator for Shear Correlation Functions

Let us now use this catalogue to measure correlation functions, which is the whole essence of a WL survey in order to constrain Cosmology. We start by using the usual estimator for shear correlation functions given by equation (2.184). The catalogue that we use contains a bit more than three million points. We therefore realise that performing calculations with such a huge dataset can be proved quite time consuming. However, there is a code that can handle such a huge dataset and give a result within a few minutes. This amazing code was developed by Mike Jarvis [55], it carries the name "*TreeCorr*" and can be found on GitHub following this link `https://rmjarvis.github.io/TreeCorr/_build/html/index.html`. It can compute shear-shear correlation functions, cross-correlation functions and other two-point statistics. For our project, we are interested in shear-shear correlations (for the usual estimator) and in cross correlations (for the optimal estimator, as we shall see in 4.3).

Let us explain briefly how one can use this code for calculating shear-shear correlation functions. First of all, we have to define a catalogue in TreeCorr, that will contain the appropriate elements

for our calculations. These elements are:

- **Coordinates :** We need to specify the coordinate system that we are using. In our case we are using x- and y- coordinates and not right ascension and declination
- **Shear Components :** According to (2.184), we need the tangential and the cross components of ellipticity. In TreeCorr, all we need to do, is to specify the so-called $g1$ and $g2$ components, which for the usual estimator are the $\epsilon_{obs,1}$ and $\epsilon_{obs,2}$ components. The code will then do the rest and compute tangential and cross components.
- **Units :** Specify the unit system. In our case is *arcmin*

Once this is done, we specify to the code which correlation function to use and we define the binning. This is done by specifying the minimum and maximum separations, the bin size and the units which in our case are *arcmin*. We choose the minimum separation to be 1 and the maximum separation to be 100, while the bin size is 0.1. The next step is to define the separation and then the code will compute the ξ_+ and the ξ_- functions.

Let us show the calculation for the shear-shear correlation function, for which we used the shear values given by the catalogue, *i.e.* we set $g1 = \gamma_1$ and $g2 = \gamma_2$. The calculation is hosted on `https://github.com/Chrisostomos-Stamou/Combining-Weak-Lensing-and-Galaxy-Light-Polarisation` in the file "Usual Correlation Function.ipynb".

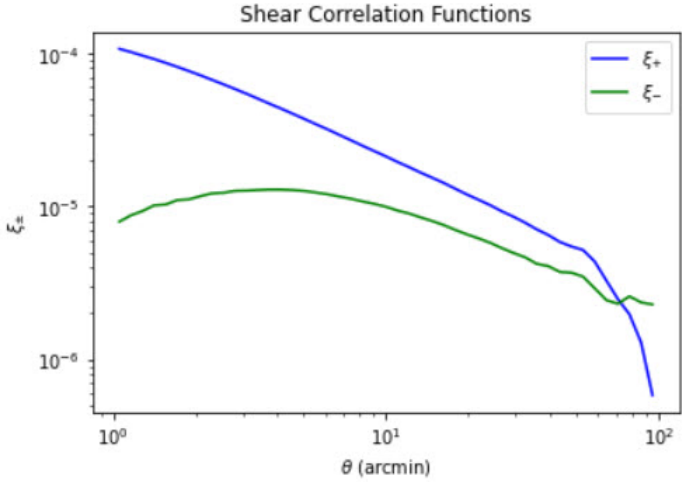

Figure 19: Shear correlation functions $\xi_\pm$ for the KiDS-450 Mock Source catalogue.

As we can see from figure 19, the shear correlation function drops as the separation increases. This behaviour makes absolute sense, since the greater the separation the less the number of galaxies that are close enough to be correlated. We should mention here, that this is not what is actually measured in an observation. Here, we exploited the simulated data sets that provide us with the shear values to see how the noise-free correlation function should look like. This way, we have

defined a "reference frame" according to which we can test if the noise of the optimal estimator is less than the noise of the ellipticity estimator given in (2.184).

4.3 Construction and Computation of the Optimal Estimator for Shear Correlation Functions

Recall that the goal of the project is to investigate if polarisation can carry some extra information on WL surveys and we are now in position to finally check this in the proper way. We begin by constructing an optimal estimator for shear correlation functions. This is done by substituting equation (3.18) into equation (2.184):

$$\xi_{\pm} = \langle \Gamma_{opt,t} \Gamma'_{opt,t} \rangle \pm \langle \Gamma_{opt,\times} \Gamma'_{opt,\times} \rangle$$

where the prime denotes the source located at the separation. From now on we drop the subscript *obs*, and every time we write ϵ we mean observed ellipticity, unless it is otherwise stated. We thus have:

$$\xi_{\pm}^{opt} = \left\langle \left(\epsilon_t - \frac{P\sigma_e^2}{\sigma_p^2 + P^2\sigma_e^2} p_t \right) \left(\epsilon'_t - \frac{P\sigma_e^2}{\sigma_p^2 + P^2\sigma_e^2} p'_t \right) \right\rangle \pm \left\langle \left(\epsilon_\times - \frac{P\sigma_e^2}{\sigma_p^2 + P^2\sigma_e^2} p_\times \right) \left(\epsilon'_\times - \frac{P\sigma_e^2}{\sigma_p^2 + P^2\sigma_e^2} p'_\times \right) \right\rangle$$

To tide up a bit the latter expression, we set $\zeta = \frac{P\sigma_e^2}{\sigma_p^2 + P^2\sigma_e^2}$. Expanding the equation yields:

$$\Rightarrow \xi_{\pm}^{opt} = \left[\langle \epsilon_t \epsilon'_t \rangle - \zeta \langle \epsilon_t p'_t \rangle - \zeta \langle p_t \epsilon'_t \rangle + \zeta^2 \langle p_t p'_t \rangle \right] \pm \left[\langle \epsilon_\times \epsilon'_\times \rangle - \zeta \langle \epsilon_\times p'_\times \rangle - \zeta \langle p_\times \epsilon'_\times \rangle + \zeta^2 \langle p_\times p_\times \rangle \right] \quad (4.1)$$

If we look carefully at this expression, we see that the right-hand-side contains the following four different correlation functions:

- The *usual shear correlation function*:

$$\xi_{\pm}^{usual} = \langle \epsilon_t \epsilon'_t \rangle \pm \langle \epsilon_\times \epsilon'_\times \rangle \quad (4.2)$$

- A *Polarisation Correlation Function*:

$$\xi_{\pm}^{pol} = \langle p_t p'_t \rangle \pm \langle p_\times p_\times \rangle \quad (4.3)$$

- *Two cross-correlation functions between observed ellipticity and polarisation*:

$$\xi_{\pm}^{ep} = \langle \epsilon_t p'_t \rangle \pm \langle \epsilon_\times p'_\times \rangle \qquad \& \qquad \xi_{\pm}^{pe} = \langle p_t \epsilon'_t \rangle \pm \langle p_\times \epsilon'_\times \rangle \quad (4.4)$$

  Notice that those two functions are equal, because we are averaging over the same galaxy pairs.

Substituting these equations into (4.1) we obtain:

$$\boxed{\xi_{\pm}^{opt} = \xi_{\pm}^{usual} + \left[\frac{P\sigma_e^2}{\sigma_p^2 + P^2\sigma_e^2}\right]^2 \xi_{\pm}^{pol} - \frac{P\sigma_e^2}{\sigma_p^2 + P^2\sigma_e^2}\left(\xi_{\pm}^{ep} + \xi_{\pm}^{pe}\right)} \tag{4.5}$$

The next step is to compute the shear correlation functions by using the optimal estimator that we just derived for different values of P, and a fixed $\sigma_p = 0.25$. We wish to test if the variance of this estimator is smaller than the variance of the usual estimator given by (2.184). We thus calculate both of the estimators, and we check the difference between their variances for different values of P. The code for this calculation can be also found on the GitHub repository `https://github.com/Chrisostomos-Stamou/Combining-Weak-Lensing-and-Galaxy-Light-Polarisation` in the file "Opt_Shear_corrf.ipynb".

We first present a plot where the difference between the estimator using ellipticity and the estimator using shear (see figure 19) are shown:

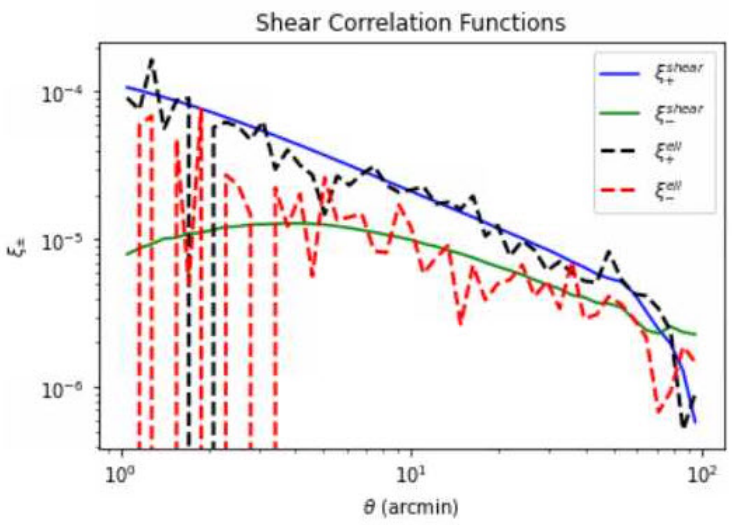

Figure 20: Shear correlation functions after using observed ellipticity (dashed lines) and the given shear values (solid lines).

We realise from this figure that observed ellipticity is a noisy estimator for shear and we hence expect the estimator containing polarisation to reduce this noise. The process for computing the optimal estimator is the same as we did for the usual one, but now we have to include cross correlations. TreeCorr is also capable of performing such operations and all we have to do is to define two catalogues, one where the $g1$ and $g2$ components are the observed ellipticities and one where the $g1$ and $g2$ are the polarisations. Then, TreeCorr can cross-correlate them.

Taking all these into account, we computed the optimal estimator for ten different values of P and a fixed σ_p. Then, we plotted the variance of the optimal estimator, the variance of the usual

estimator using the observed ellipticity and the variance of the usual estimator using shear. The result is shown in figure 21.

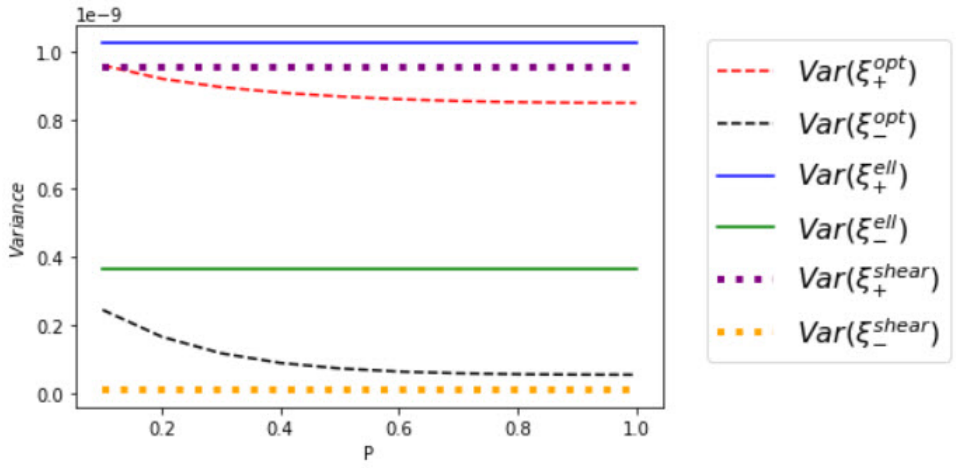

Figure 21: Comparison among the variances of the three estimators that we used for computing shear correlation functions.

The optimal estimators are represented by the dashed lines and we can clearly see that the variance of the optimal estimator drops while P increases and it is smaller than the variance of the usual estimator represented by solid lines. We thus prove that a correlation between polarisation and intrinsic ellipticity with a strength given by the value of P would reduce the shape noise provided by the observed ellipticity estimator. We also include the variance in the estimator using the given shear values. We see that the variance of ξ_+ is smaller than the variance of ξ_-, which means that the simulated data give a more accurate computation for ξ_+ than they give for ξ_-, something that can be also seen in figure 20.

Let us finally make explicit the noise that each estimator brings to the measurement by calculating the following two quantities:

- Variance of the difference between the optimal estimator minus the noise-free shear correlation function:
$$Var\left[\frac{\xi_\pm^{opt} - \xi_\pm^{shear}}{\sigma_e}\right]$$
where we divided by the shape noise to normalise the variance.
- Variance of the difference between the ellipticity estimator minus the noise-free shear correlation function:
$$Var\left[\frac{\xi_\pm^{ell} - \xi_\pm^{shear}}{\sigma_e}\right]$$

Let us plot the results for the different values of P. The results are shown in figure 22. It is clear

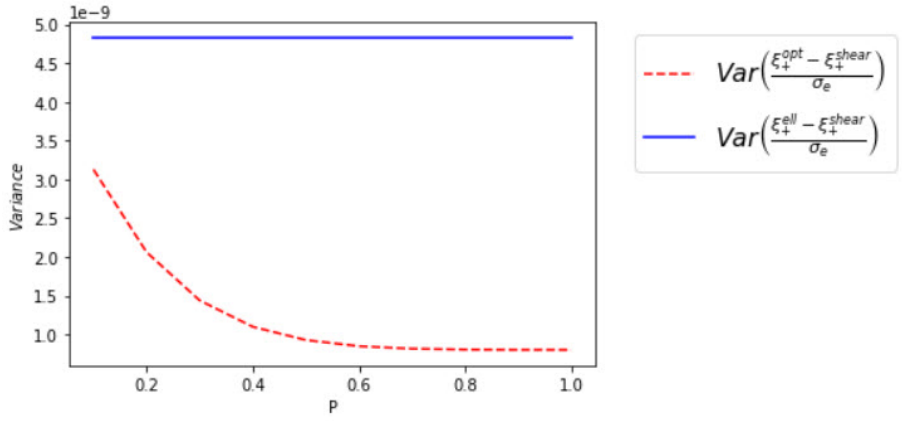

(a) Comparison of the noise of the plus component between the optimal and ellipticity estimators.

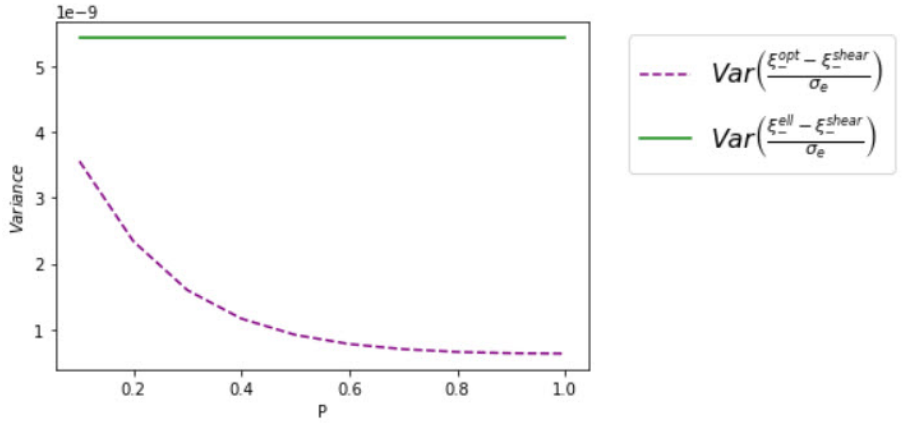

(b) [Comparison of the noise of the minus component between the optimal and ellipticity estimators

Figure 22: Comparison of the noise between the optimal and ellipticity estimators

that the optimal estimator is less noisy than the estimator using ellipticity and this noise drops as the strength of the correlation between polarisation and intrinsic ellipticity, *i.e.* the value of P, increases.

5 Conclusions

The present Thesis investigated how polarisation and weak lensing can be optimally combined in order for polarisation to reduce some of the shape noise, and it was motivated by the fact that weak lensing is a versatile cosmological probe. We therefore started in Chapter 1 by introducing the concept of the project and briefly reviewing how weak lensing can be used to constrain cosmology. We then moved on to Chapter 2, where we studied in depth weak lensing and specifically the Cosmic Shear case, for which we derived all the involved equations and we made explicit the connection to Cosmology. Afterwards, we started the research part of the project in Chapter 3, where we constructed an optimal estimator for measuring shear that includes polarisation (3.18). We then put it to test by a "naive" numerical simulation, where we generated random catalogues of galaxies and tested the effect of polarisation to weak lensing. We proved for this simulation that if polarisation and intrinsic ellipticity are correlated- a correlation characterised by the parameter P- the variance of the optimal estimator is less than the variance of the usual one. Finally, in Chapter 4 we used an actual numerical simulation provided by SLICS, in which galaxies are sheared by a dark matter distribution and we verified our results of Chapter 3 by repeating the same process. Then, we simulated an actual research by measuring shear correlation functions and testing the effect of polarisation to weak lensing. Since the catalogue provided by SLICS gives both shear and observed ellipticity, we were capable of measuring shear correlation functions by using the actual shear components, *i.e.* a noise-free estimator, and compare it to the estimator that includes ellipticity and the optimal estimator including polarisation. This way, we could identify which estimator is less noisy and we proved that the optimal estimator brings less noise to the shear measurement (see figure 22). We finally mention that the codes used for the above calculations are publicly available on GitHub, following the link: `https://github.com/Chrisostomos-Stamou/Combining-Weak-Lensing-and-Galaxy-Light-Polarisation`.

ACKNOWLEDGEMENTS

I would like to thank my main supervisor for this project, Dr. Koen Kuijken, for giving me the opportunity to work with him on an interesting project and for all his advice and comments that helped me enhance my theoretical and computational skills. I am also grateful to Dr. Fabrizio Renzi for his important help on understanding some crucial for my project concepts and finally, I would like to thank Dr. Matthieu Schaller, who kindly agreed to co-supervise my project.

References

[1] M. Meneghetti, *Introduction to Gravitational Lensing: With Python Examples*, vol. 956. Springer Nature, 2021.

[2] P. Schneider, "Gravitational lensing statistics," in *Gravitational Lenses*, pp. 196–208, Springer, 1992.

[3] A. B. Congdon and C. R. Keeton, *Principles of Gravitational Lensing*. Springer, 2018.

[4] S. Dodelson, *Gravitational lensing*. Cambridge University Press, 2017.

[5] M. P. Hobson, G. P. Efstathiou, and A. N. Lasenby, *General relativity: an introduction for physicists*. Cambridge University Press, 2006.

[6] S. M. Carroll, *Spacetime and geometry*. Cambridge University Press, 2019.

[7] C. W. Misner, K. S. Thorne, and J. A. Wheeler, *Gravitation*. Macmillan, 1973.

[8] J. B. Hartle, "Gravity: an introduction to einstein's general relativity," 2003.

[9] R. A. d'Inverno, "Introducing einstein's relativity," *Introducing Einstein's relativity by RA D'Inverno. New York: Oxford University Press*, 1992.

[10] L. Ryder, *Introduction to general relativity*. Cambridge University Press, 2009.

[11] F. W. Dyson, A. S. Eddington, and C. Davidson, "Ix. a determination of the deflection of light by the sun's gravitational field, from observations made at the total eclipse of may 29, 1919," *Philosophical Transactions of the Royal Society of London. Series A, Containing Papers of a Mathematical or Physical Character*, vol. 220, no. 571-581, pp. 291–333, 1920.

[12] M. Bartelmann and P. Schneider, "Weak gravitational lensing," *Physics Reports*, vol. 340, no. 4-5, pp. 291–472, 2001.

[13] D. Walsh, R. F. Carswell, and R. J. Weymann, "0957+ 561 a, b: twin quasistellar objects or gravitational lens?," *Nature*, vol. 279, no. 5712, pp. 381–384, 1979.

[14] T. Treu and P. J. Marshall, "Time delay cosmography," *The Astronomy and Astrophysics Review*, vol. 24, no. 1, pp. 1–41, 2016.

[15] S. H. Suyu, T. Treu, S. Hilbert, A. Sonnenfeld, M. W. Auger, R. D. Blandford, T. Collett, F. Courbin, C. D. Fassnacht, L. V. Koopmans, *et al.*, "Cosmology from gravitational lens time delays and planck data," *The Astrophysical Journal Letters*, vol. 788, no. 2, p. L35, 2014.

[16] M. Irwin, R. Webster, P. Hewett, R. Corrigan, and R. Jedrzejewski, "Photometric variations in the q2237+ 0305 system-first detection of a microlensing event," *The Astronomical Journal*, vol. 98, 1989.

[17] J. A. Tyson, F. Valdes, and R. Wenk, "Detection of systematic gravitational lens galaxy image alignments-mapping dark matter in galaxy clusters," *The Astrophysical Journal*, vol. 349, pp. L1–L4, 1990.

[18] C. Heymans, L. Van Waerbeke, L. Miller, T. Erben, H. Hildebrandt, H. Hoekstra, T. D. Kitching, Y. Mellier, P. Simon, C. Bonnett, *et al.*, "Cfhtlens: the canada–france–hawaii telescope lensing survey," *Monthly Notices of the Royal Astronomical Society*, vol. 427, no. 1, pp. 146–166, 2012.

[19] L. Van Waerbeke, J. Benjamin, T. Erben, C. Heymans, H. Hildebrandt, H. Hoekstra, T. D. Kitching, Y. Mellier, L. Miller, J. Coupon, *et al.*, "Cfhtlens: mapping the large-scale structure with gravitational lensing," *Monthly Notices of the Royal Astronomical Society*, vol. 433, no. 4, pp. 3373–3388, 2013.

[20] K. Kuijken, C. Heymans, H. Hildebrandt, R. Nakajima, T. Erben, J. T. De Jong, M. Viola, A. Choi, H. Hoekstra, L. Miller, *et al.*, "Gravitational lensing analysis of the kilo-degree survey," *Monthly Notices of the Royal Astronomical Society*, vol. 454, no. 4, pp. 3500–3532, 2015.

[21] J. T. De Jong, G. A. V. Kleijn, D. R. Boxhoorn, H. Buddelmeijer, M. Capaccioli, F. Getman, A. Grado, E. Helmich, Z. Huang, N. Irisarri, *et al.*, "The first and second data releases of the kilo-degree survey," *Astronomy & Astrophysics*, vol. 582, p. A62, 2015.

[22] M. A. Troxel, N. MacCrann, J. Zuntz, T. Eifler, E. Krause, S. Dodelson, D. Gruen, J. Blazek, O. Friedrich, S. Samuroff, *et al.*, "Dark energy survey year 1 results: Cosmological constraints from cosmic shear," *Physical Review D*, vol. 98, no. 4, p. 043528, 2018.

[23] H. Hoekstra, M. Bartelmann, H. Dahle, H. Israel, M. Limousin, and M. Meneghetti, "Masses of galaxy clusters from gravitational lensing," *Space Science Reviews*, vol. 177, no. 1-4, pp. 75–118, 2013.

[24] J.-P. Kneib and P. Natarajan, "Cluster lenses," *The Astronomy and Astrophysics Review*, vol. 19, no. 1, p. 47, 2011.

[25] M. Oguri, M. B. Bayliss, H. Dahle, K. Sharon, M. D. Gladders, P. Natarajan, J. F. Hennawi, and B. P. Koester, "Combined strong and weak lensing analysis of 28 clusters from the sloan giant arcs survey," *Monthly Notices of the Royal Astronomical Society*, vol. 420, no. 4, pp. 3213–3239, 2012.

[26] A. Zitrin, A. Fabris, J. Merten, P. Melchior, M. Meneghetti, A. Koekemoer, D. Coe, M. Maturi, M. Bartelmann, M. Postman, *et al.*, "Hubble space telescope combined strong and weak lensing analysis of the clash sample: mass and magnification models and systematic uncertainties," *The Astrophysical Journal*, vol. 801, no. 1, p. 44, 2015.

[27] M. Postman, D. Coe, N. Benitez, L. Bradley, T. Broadhurst, M. Donahue, H. Ford, O. Graur, G. Graves, S. Jouvel, *et al.*, "The cluster lensing and supernova survey with hubble: an overview," *The Astrophysical Journal Supplement Series*, vol. 199, no. 2, p. 25, 2012.

[28] K. Umetsu, E. Medezinski, M. Nonino, J. Merten, M. Postman, M. Meneghetti, M. Donahue, N. Czakon, A. Molino, S. Seitz, *et al.*, "Clash: weak-lensing shear-and-magnification analysis of 20 galaxy clusters," *The Astrophysical Journal*, vol. 795, no. 2, p. 163, 2014.

[29] K. Umetsu, A. Zitrin, D. Gruen, J. Merten, M. Donahue, and M. Postman, "Clash: Joint analysis of strong-lensing, weak-lensing shear, and magnification data for 20 galaxy clusters," *The Astrophysical Journal*, vol. 821, no. 2, p. 116, 2016.

[30] J. Lotz, A. Koekemoer, D. Coe, N. Grogin, P. Capak, J. Mack, J. Anderson, R. Avila, E. Barker, D. Borncamp, *et al.*, "The frontier fields: survey design and initial results," *The Astrophysical Journal*, vol. 837, no. 1, p. 97, 2017.

[31] B. Salmon, D. Coe, L. Bradley, R. Bouwens, M. Bradač, K.-H. Huang, P. A. Oesch, D. Stark, K. Sharon, M. Trenti, *et al.*, "Relics: the reionization lensing cluster survey and the brightest high-z galaxies," *The Astrophysical Journal*, vol. 889, no. 2, p. 189, 2020.

[32] H. Ebeling, A. Edge, and J. Henry, "Macs: A quest for the most massive galaxy clusters in the universe," *The Astrophysical Journal*, vol. 553, no. 2, p. 668, 2001.

[33] A. von der Linden, M. T. Allen, D. E. Applegate, P. L. Kelly, S. W. Allen, H. Ebeling, P. R. Burchat, D. L. Burke, D. Donovan, R. G. Morris, *et al.*, "Weighing the giants–i. weak-lensing masses for 51 massive galaxy clusters: project overview, data analysis methods and cluster images," *Monthly Notices of the Royal Astronomical Society*, vol. 439, no. 1, pp. 2–27, 2014.

[34] P. L. Kelly, A. von der Linden, D. E. Applegate, M. T. Allen, S. W. Allen, P. R. Burchat, D. L. Burke, H. Ebeling, P. Capak, O. Czoske, *et al.*, "Weighing the giants–ii. improved calibration of photometry from stellar colours and accurate photometric redshifts," *Monthly Notices of the Royal Astronomical Society*, vol. 439, no. 1, pp. 28–47, 2014.

[35] D. E. Applegate, A. von der Linden, P. L. Kelly, M. T. Allen, S. W. Allen, P. R. Burchat, D. L. Burke, H. Ebeling, A. Mantz, and R. G. Morris, "Weighing the giants–iii. methods and measurements of accurate galaxy cluster weak-lensing masses," *Monthly Notices of the Royal Astronomical Society*, vol. 439, no. 1, pp. 48–72, 2014.

[36] A. B. Mantz, A. Von der Linden, S. W. Allen, D. E. Applegate, P. L. Kelly, R. G. Morris, D. A. Rapetti, R. W. Schmidt, S. Adhikari, M. T. Allen, *et al.*, "Weighing the giants–iv. cosmology and neutrino mass," *Monthly Notices of the Royal Astronomical Society*, vol. 446, no. 3, pp. 2205–2225, 2015.

[37] G. Hinshaw, D. Larson, E. Komatsu, D. N. Spergel, C. Bennett, J. Dunkley, M. Nolta, M. Halpern, R. Hill, N. Odegard, *et al.*, "Nine-year wilkinson microwave anisotropy probe (wmap) observations: cosmological parameter results," *The Astrophysical Journal Supplement Series*, vol. 208, no. 2, p. 19, 2013.

[38] P. A. Ade, N. Aghanim, C. Armitage-Caplan, M. Arnaud, M. Ashdown, F. Atrio-Barandela, J. Aumont, C. Baccigalupi, A. J. Banday, R. Barreiro, *et al.*, "Planck 2013 results. xv. cmb power spectra and likelihood," *Astronomy & Astrophysics*, vol. 571, p. A15, 2014.

[39] L. Van Waerbeke, Y. Mellier, T. Erben, J. Cuillandre, F. Bernardeau, R. Maoli, E. Bertin, H. Mc Cracken, O. L. Fevre, B. Fort, *et al.*, "Detection of correlated galaxy ellipticities on cfht data: first evidence for gravitational lensing by large-scale structures," *Arxiv preprint astro-ph/0002500*, 2000.

[40] D. M. Wittman, J. A. Tyson, D. Kirkman, I. Dell'Antonio, and G. Bernstein, "Detection of weak gravitational lensing distortions of distant galaxies by cosmic dark matter at large scales," *nature*, vol. 405, no. 6783, pp. 143–148, 2000.

[41] D. J. Bacon, A. R. Refregier, and R. S. Ellis, "Detection of weak gravitational lensing by large-scale structure," *Monthly Notices of the Royal Astronomical Society*, vol. 318, no. 2, pp. 625–640, 2000.

[42] H. Hildebrandt, M. Viola, C. Heymans, S. Joudaki, K. Kuijken, C. Blake, T. Erben, B. Joachimi, D. Klaes, L. t. Miller, *et al.*, "Kids-450: Cosmological parameter constraints from tomographic weak gravitational lensing," *Monthly Notices of the Royal Astronomical Society*, vol. 465, no. 2, pp. 1454–1498, 2017.

[43] T. Abbott, F. B. Abdalla, A. Alarcon, J. Aleksić, S. Allam, S. Allen, A. Amara, J. Annis, J. Asorey, S. Avila, *et al.*, "Dark energy survey year 1 results: Cosmological constraints from galaxy clustering and weak lensing," *Physical Review D*, vol. 98, no. 4, p. 043526, 2018.

[44] H. Aihara, N. Arimoto, R. Armstrong, S. Arnouts, N. A. Bahcall, S. Bickerton, J. Bosch, K. Bundy, P. L. Capak, J. H. Chan, *et al.*, "The hyper suprime-cam ssp survey: overview and survey design," *Publications of the Astronomical Society of Japan*, vol. 70, no. SP1, p. S4, 2018.

[45] K. Wood and T. J. Jones, "Modeling polarization maps of external galaxies.," *The Astronomical Journal*, vol. 114, p. 1405, 1997.

[46] E. Audit and J. F. Simmons, "The use of light polarization in weak-lensing inversions," *Monthly Notices of the Royal Astronomical Society*, vol. 303, no. 1, pp. 87–95, 1999.

[47] N. Okabe, M. Takada, K. Umetsu, T. Futamase, and G. P. Smith, "Locuss: Subaru weak lensing study of 30 galaxy clusters," *Publications of the Astronomical Society of Japan*, vol. 62, no. 3, pp. 811–870, 2010.

[48] D. Baumann, "Cosmology," *Part III Mathematical Tripos*, 2012.

[49] H. Mo, F. Van den Bosch, and S. White, *Galaxy formation and evolution*. Cambridge University Press, 2010.

[50] L. Verde, "Statistical methods in cosmology," in *Lectures on Cosmology*, pp. 147–177, Springer, 2010.

[51] T. Robishaw and C. Heiles, "The measurement of polarization in radio astronomy," in *The WSPC Handbook of Astronomical Instrumentation: Volume 1: Radio Astronomical Instrumentation*, pp. 127–158, World Scientific, 2021.

[52] K. Wood, "Scattering and dichroic extinction: Polarimetric signatures of galaxies," *The Astrophysical Journal*, vol. 477, no. 1, p. L25, 1997.

[53] J. F. Simmons and E. Audit, "The optical polarization of spiral galaxies," *Monthly Notices of the Royal Astronomical Society*, vol. 319, no. 2, pp. 497–509, 2000.

[54] C. Packham, S. Young, and D. Axon, "Polarimetry of galactic discs: A brief review," *Astronomical Polarimetry 2008: Science from Small to Large Telescopes*, vol. 449, p. 405, 2011.

[55] M. Jarvis, "Treecorr: Two-point correlation functions," *Astrophysics Source Code Library*, pp. ascl–1508, 2015.